Deanship of Graduate Studies
Al – Quds University

Zeta potential of electric double layer for dendrimers: Monte Carlo simulation study

Aya Ibrahim Mosa Ja'freh

M.Sc. Thesis

Jerusalem – Palestine

1445/2023

Zeta potential of electric double layer for dendrimers: Monte Carlo simulation study

Prepared by:

Aya Ibrahim Mosa Ja'freh

B.Sc. in Medical Laboratory

Sciences from Al-Quds University/Palestine

Supervisor: Dr. Khawla Qamhieh

Thesis submitted in partial fulfillment of requirement for the degree of Master of Biochemistry And Molecular in Faculty of Medicine Department\ Al-Quds University

1445/2023

Deanship of Graduate Studies
Al – Quds University
Department of medicine

Thesis approval

Zeta potential of electric double layer for dendrimers: Monte Carlo simulation study

Prepared by: Aya Ibrahim Mosa Ja'freh

Registration No: 22012471

Supervisor: Dr. Khawla Qamhieh

Master thesis submitted and accepted date 28/ 11/2023

The name and signature of examining committee member are as follows:

1. Head of the committee: Dr. Khawla Qamhieh Signature: ... …… …

2. Internal Examiner: Dr.Wadie Sultan Signature: ... .

3. External Examiner: Dr. Jamal Ghabboun Signature:

1445/2023

Dedication

I dedicate this thesis to my father and mother.
To my sisters and brothers.
To my husband.
To my little son.
To my teachers.

Aya Ja'freh

Declaration:

I certify that this thesis submitted for the degree of Master and the results found by myself, except where otherwise acknowledged, and that this study has not been submitted for a higher degree to any other university or institution.

Signature: 

Aya Ibrahim Mosa Ja'freh

Date: 28/ 11/ 2023

Zeta potential of electric double layer for dendrimers: Monte Carlo simulation study.

Prepared by: Aya Ja'freh.

Supervisors: Dr. Khawla Qamheih

Abstract

In this study, the potential of the electric double layer (EDL) of different generations of dendrimers in a spherical boundary system has been studied using Monte Carlo (MC) simulations. The effects of Changing the dielectric constant of the solvent, the charge and the radius of generations from G1 to G8, have been studied.

The radial distribution function between dendrimer and counterions, running coordination number, integrated charge number, Z effective, zeta and surface potentials were plotted as results of simulation methods.

Dendrimers possess a higher electrostatic potential near their surfaces, it increases with the increase of the counterions and the values of distributed ions and accumulated charge increase when the generation of Dendrimers increase.

An observed correlation indicates that as generation increases, there's a simultaneous rise in the zeta potential of the electric double layer and the surface potential. This concurrent increase leads to a higher effective charge (Zeff) within the positive region, suggesting elevated charge accumulation.

With the dielectric constant =10 that represents the cytoplasm, the interaction between dendrimer and counterions increases, as well as the accumulation near the surface that increases too. Moreover, the electrostatic correlation, the accumulated charge and the magnitude of the electrostatic potential increase with increasing the generation of Dendrimers. The surface potential increases as the generation of the dendrimer increase. However, the values of zeta potential decrease as generation of Dendrimers increase.

Table of contents

List of tables

List of Figures

List of Abbreviations

DNA Deoxyribonucleic acid

PAMAM Poly(amido amine)

lp The persistence length

DLVO The Derjaguin-Landau-Verwey-Overbeek theory.

Nc number of core

Nb number of branch

PII Poly(propylene imine)

PH Potential of Hydrogen

EDL The electrical double layer.

DLVO The Derjaguin-Landau-Verwey-Overbeek theory.

ZP Zeta potential

ζ Zeta

LDV laser doppler velocimetry

MC Monte Carlo

EDL electric double layer

Z_I The charge of the counterions.

Z_M The charge of macroion.

R_I The radius of the counterions.

R_M The radius of macroion.

N_m number of macroion

ε_r relative static permittivity

T The temperature =298 K in Kelvin.

NVT Canonical ensemble, constant number of particles (N)
, temperature (T) ,and volume (V)

R_{sph} radius of sphere

U Total potential.

U_{hs} Hard-sphere repulsion.

U_{elec} Coulomb interaction.

U_{ext} External potential.

ρM Macroion number density.

ΦM Macroion volume fraction.

e is the elementary charge.

RDFs Radial Distribution Functions

RCN Running Coordination Number

Å Angstrom.

Chapter One

Introduction

1.1 Introduction

It's important to create and develop new applications and techniques in order to discover pivotal and successful treatments for various human diseases.
The delivery of a medicine to the site of action is a major challenge in the treatment of many diseases. (Nomani et al.,2010)

In the past decade, gene therapy has emerged as a promising solution for diseases where effective drug treatments are limited. Researchers have identified numerous targets for gene therapy to deliver genetic materials in vivo, marking significant progress in this field. (Keiji and Kazunori ,2009)

It is possible to deliver genes via viral and non-viral vectors. It is well known that viral vectors are efficient at delivering genes to target cells but the biggest concerns are their putative cytotoxicity and unidentified long-term effects. A non-viral vector's lower immunogenicity, increased safety, and simplicity of preparation make it an attractive alternative to viral vectors (i.e., chemical), including systems made of cationic lipids (lipoplexes) and cationic polymers (polyplexes). However, the majority of these systems continue to be ineffective and limited. Nanoparticles, a new non-viral vector, have received attention recently because of their important characteristics, including a surface effect, a small size effect, lower immunogenicity, improved safety, and ease of preparation. (Dendrimers) are incredibly effective at delivering genetic material into cells, particularly in vitro. By creating an effective synthesis and modification procedure, the dendrimer's size, shape, and surface functioning may be accurately regulated. A well-designed synthesis method results in monodisperse structures for the final products. (Qamhieh and Khaleel, ,2014)

Within cells, DNA, a double-stranded molecule that forms a double helix, transports genetic information. With sugar groups and phosphoric acid groups in the backbone of the DNA molecule's two strands, the molecule has a net negative charge.

The genetic code is made up of the bases of the two complementary strands. DNA is an effective polyelectrolyte with repeating negatively charged units that are assumed to be amphiphilic. The extended conformation of DNA in aqueous solutions is caused by its strongly negative charge, and its persistence length (lp), which is around 50 nm, serves as a measure of molecular stiffness. DNA in the nucleus of eukaryotic cells is folded into the highly organized chromatin structure. (Zinchenko and Chen,2006)

DNA is essential for a living organism's function and information storage, In order to treat diseases, DNA must be compressed and delivered into the inside of cell nuclei, a process that is seen in the practical applications of gene therapy and antisense therapy. (Schiessel, 2003)

For transfection, the targeted DNA is combined with the activated PAMAM-dendrimers. The interaction between the positively charged amino groups situated on the dendrimer molecule's surface and the negatively charged phosphate groups of the DNA molecule results in the formation of a DNA-dendrimer complex known as a dendriplex. This complex exhibits a toroid-like structure, it is transported to the specific cell via the bloodstream. DNA molecules are tightly packed together within the complex. Due to their positive net charge, they possess the capability to bind with negatively charged surface molecules. Specifically, on the membranes of eukaryotic cells, these entities, also with a positive net charge, can effectively bind to the negatively charged surface molecules. (Ma,2013)

Afterwards an endosome escape is required; otherwise, the dendriplex will breakdown after endosome and lysosome fusion. The primary route for internalization inside the cytoplasm is endosome uptake. Another essential step is the movement of gene materials from the cytoplasm to the nucleus. (Jörg and Emma, 2002)

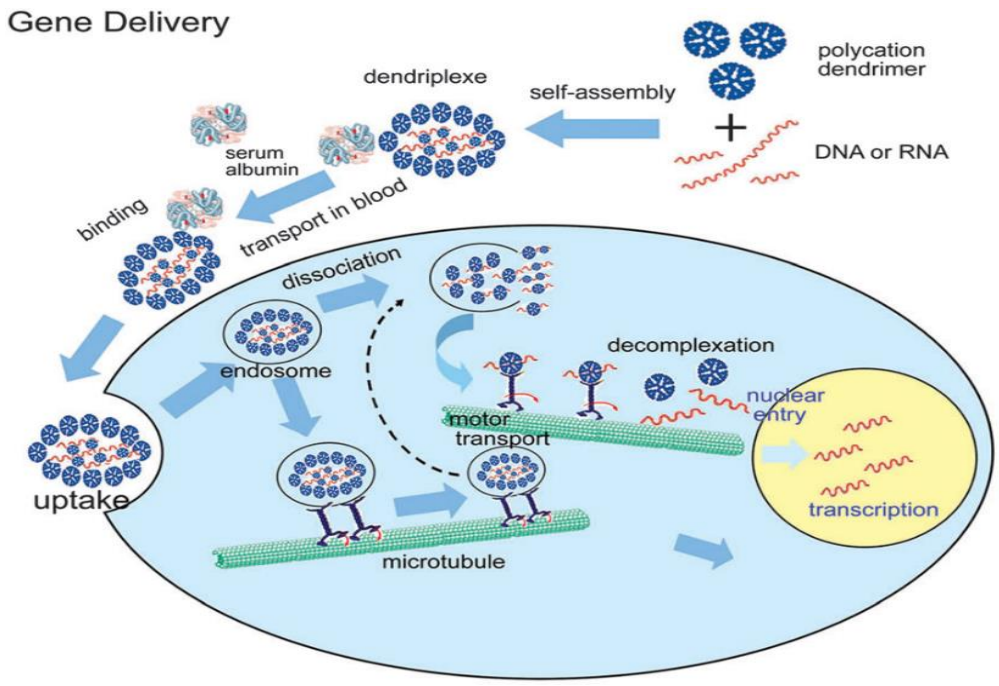

Figure1.1: Sketch of the gene transfection process with dendrimers: a model system of bioactive molecule delivery.

1.2 Colloids

The term “colloid” which means glue in Greek, is derived from that word. When Thomas Graham conducted osmosis and diffusion research in 1860, he discovered gelatinous polymer colloids that were the first to be utilized for it. (Hunter,2013)

Colloids arewidely present in nature and various industrial applications like fog, smoke, paint, milk, and ink, consist of small solid or liquid particles dispersed in a different medium, air or another liquid. One defining characteristic that separates colloidal solutions from molecular or basic electrolyte solutions, such as sugar or salt solutions, is the substantial difference in size and mass between the colloidal particles and the solvent molecules or microscopic ions Colloids are particles of mesoscopic or even nanoscopic scale, ranging from a few nanometers to microns in size. While they are composed of numerous atoms, they lack the sufficient quantity to exhibit bulk-like behavior. (Vogel et al., 2015)

The stability of colloidal dispersions relies on the DLVO theory, which explains how long-range repulsive interactions between colloidal particles occur. By charging the surfaces of these particles, they repel each other, preventing aggregation and ensuring stability. This mechanism is vital in various applications such as food emulsions like milk, where the prevention of large aggregates and sedimentation is essential for product quality and shelf life. (Naji *et al*., 2010).

1.3 Dendrimers

The term "dendrimer" originates from the Greek lexicon, from the words "dendron" which translates to "tree" or "branch". Dendrimers are a class of nanostructured macromolecules (Anupa, 2010), regularly branched polymers with a dendritic, treelike structure (Mansfield et al.,1993). They are described in terms of generations defined as the number of branching points when going from the core towards the periphery of the dendrimer, each generation being represented by an additional ‘‘shell’’ on the dendrimer surface, going into their structure (Sherje et al.,2018) Dendrimers stand out due to their distinctive molecular structure characterized by nanoscale uniform size, high branching, polyvalency, water solubility, internal cavities, and accessible synthesis methods. These unique properties make dendrimers highly versatile in biomedical research. They find extensive use as carrier systems for therapeutic drugs and delivery methods for therapeutic compounds due to their tailored structure, enabling controlled and targeted delivery for enhanced biomedical applications, also in diagnostics, and biomedical engineering. (Kimet al,2018) (Keerti et al,2020)

Dendrimers exhibit a distinct architectural arrangement comprising three primary components: an interior core, interior layers formed by repeating units connected radially to the core, and an

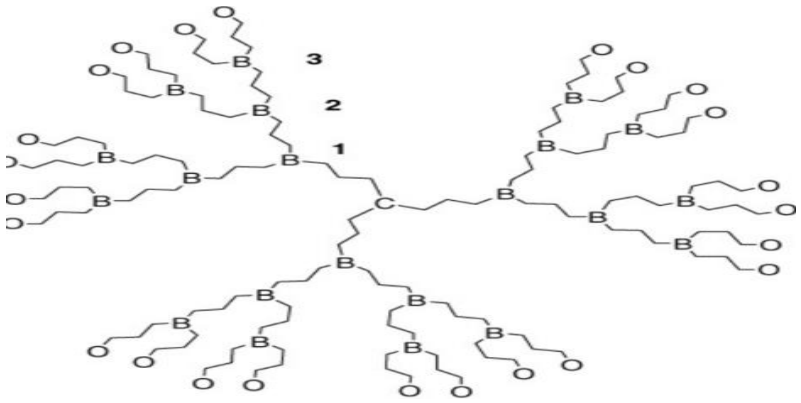

outermost layer, termed terminal functionality, attached to the final interior generation. This unique structure is fundamental to the diverse applications of dendrimers, particularly in biomedical research and various innovative fields.(Dias et al,2020). Dendrimer generation is defined as the hyperbranching of a dendrimer as it moves from its center to its periphery, resulting in homostructural layers between the focal points (branching points). The generation number is the number of focal points while going from the core to the dendrimer surface; for example, when looking from the center to the outward, a dendrimer with five focal points is called a G5-dendrimer. (Tripathy and Das,2013)

Figure 1.2: The dendrimer is a polymer characterized by a central core (C), branching points (B), and outer surface groups (O).

In accordance with the information provided by Tomalia in 2005, as dendrimer generation (G) increases, the size of the dendrimer grows linearly. The number of functional primary amine groups (Z) on the surface of the dendrimer follows an exponential increase, calculated as $Z = Nc * Nb^G$. In this equation, Nc represents the core multiplicity, which is 4 for ethylenediamine and 3 for ammonia. Additionally, Nb denotes the branch cell multiplicity, which is 2 for both cases (see figure 1). For example, a Generation 2 (G2) dendrimer with an ethylenediamine core and poly (amido amine) (PAMAM) structure would contain Z = 4 * 2^2 = 16 surface amine groups at a neutral pH. Table 1.1 displays the number of surface groups for (G0 - G10).

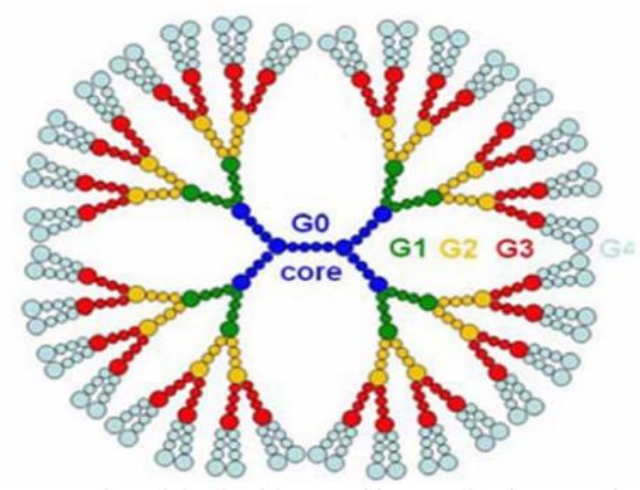

Figure 1.3: The dendrimer architecture illustrated with a tetrafunctional core (Nc = 4) and bifunctional branches (Nb = 2).

Table 1.1: theoretical properties of Polvamidoamine dendrimers.

Generation	Number of terminal groups	
	Ammonia cored PAMAM dendrimer	Ethylenediamine cored PAMAM dendrimer
0	3	4
1	6	8
2	12	16
3	24	32
4	48	64
5	96	128
6	192	256
7	384	512
8	768	1024
9	1536	2048
10	3072	4096

1.3.1 Types of Dendrimers

There are many types of Dendrimers and they are represented asby:

- **PAMAM** Dendrimer which is the most familiar dendrimer is Poly (amidoamine), whose fundamental element is trivalent nitrogen.
- **PPI** Dendrimer**,** The polypropylene imines in it are polyalkyl amines with primary amine groups as their end groups.
- **Tecto** Dendrimer is an intelligent therapeutic nanodevice that must be capable of performing a number of functions, including diagnosis, drug delivery, and recognizing diseased cells.
- **Multilingual** Dendrimers have several copies of a particular functional group present on the surface of these dendrimers.
- **Hybrid** Dendrimers Linear Polymers Have properties of both linear and dendritic polymers, these are hybrid polymers.

1.3.2 Factors affecting Dendrimers properties

- Effect of pH

The dendrimer has an expanded conformation based on changes in pH. In low pH conditions, increased repulsion between positively charged amines occurs both at the dendrimer surface and in the interior. Neutral pH leads to back-folding, likely due to hydrogen bonding between uncharged tertiary amines inside and positively charged surface amines. At higher pH, dendrimers contract as the molecule becomes neutral, adopting a more spherical structure with minimized repulsive forces between arms and surface groups, resulting in a higher degree of back-folding due to weak inter-dendron repulsive forces.

- Effect of Solvent

In general, dendrimers across generations exhibit increased back-folding with reduced solvent quality or decreased solvation. Interestingly, lower generation dendrimers, owing to their greater flexibility, display a stronger inclination for back-folding in response to poor solvation compared to their higher generation counterparts. Polar dendrimers demonstrate that nonpolar aprotic solvents induce higher molecular densities in the core due to back-folding, while polar solvents solvate dendrimer arms, resulting in a higher molecular density on the dendrimer surface.

- Effect of Salt

  High salt concentrations have a significant impact on dendrimers; to reduce charge repulsion in the structure, the charged dendrimer segments are forced into an expanded conformation by repulsive forces.

- Effect of concentration

  The molecular shape of dendrimers contracts as concentration increases, making them more susceptible to being affected and sensitive to larger particles like other dendrimers or surfaces. This molecular contraction could weaken the attractive forces that bind dendrimer molecules together and increase their ability to display tighter intermolecular packing. (Samad et al,2009)

1.3.3 Dendrimer in nanomedicine and gene therapy

Dendrimers are novel polymers with molecular architectures unique among polymers, with a well-defined structure and a high degree of molecular uniformity, low polydispersity, as well as a variety of properties related to nanomedicine development. Dendrimers can deliver drugs either through complexing hydrophobic drugs inside the hydrophobic dendrimer interior or by covalently coupling drugs onto their surfaces. Dendrimers have also been shown to bypass efflux transporters. With new dendrimer-based delivery systems, drugs can be transported efficiently across cellular barriers. (Santander-Ortega et al, 2016)

The molecular architecture of dendrimers is also highly adaptable due to the easy attachment of tunable functional groups that enable chemical modifications. Their well-defined branched

molecular architecture has become an increasingly important synthetic vector for gene therapy due to its many favorable properties. The goal is to improve the gene condensation capacity, reduce toxicity, and also give the agent the ability to become stealthy or targeted after being administered. (Singh et al.,2021) (Zhao and Bau, 2009)

1.3.4 Dendrimer –drug interactions

There have been several different interaction mechanisms discovered, and they can be classified into three categories: simple encapsulations, covalent conjugations, and electrostatic interactions.

1.3.4.1 Simple Encapsulation

Dendrimers allow for direct encapsulation of guest molecules into the interior of the macromolecule due to their ellipsoidal or spheroidal form, absence of internal cavities, and open architecture. These interior spaces are empty and hydrophobic by nature, making it possible for them to interact with less-soluble medicines through hydrophobic interactions.

Additionally, by creating hydrogen bonds with the drug molecules, the nitrogen or oxygen atoms in the interior cavities can interact with them. Given these unique characteristics, interactions between medicinal molecules and dendrimer interior cavities may occur via supramolecular processes such as physical encapsulation, hydrophobic contact, or hydrogen bonding.

1.3.4.2 Covalent Conjugation

Dendrimers possess many functional groups on their surface, which makes them ideal for the covalent conjugation of many medicines with appropriate functional groups.

When drug molecules have been wrapped in hydrophobic cavities or electrostatically absorbed into the surface of dendrimers, their chemical integrity and pharmacological characteristics remain intact. However, covalent drug attachment to dendrimer surface groups via chemical

bonds gives greater control over drug release, making regulated drug delivery and tissue targeting possible.

1.3.4.3 Electrostatic Interaction

A dendrimer's surface is rich in functional groups, such as carboxyl and amine groups, which may be used to electrostatically increase the solubility of hydrophobic medicines. Ibuprofen, ketoprofen, diflunisal, naproxen, and indomethacin are just a few of the non-steroidal anti-inflammatory medicines containing carboxyl groups that have been known to complex with dendrimers through electrostatic interactions. This type of interaction has also been reported to be present in some antibacterial and anticancer medications. These drug compounds have the characteristic of being mildly acidic medications, with carboxyl groups in the molecules. (Neerman,2004)

1.3.5 Mechanism of drug delivery through dendrimers

The well-defined 3D structure and abundance of surface functional groups allow for the loading of drug molecules both inside the dendrimers and on their surface groups. In addition to interacting with drugs via electrostatic or covalent interactions at their terminal functional groups, dendrimers can also exist as drug carriers by encapsulating medications within the dendritic structure.

Two mechanisms for drug delivery:

1. The breakdown of drug dendrimer covalent bonds in vivo is dependent on enzymes or an environment that can break them.

2. The drug is released in the cavity of the receptor's core or outer shell based on changes in the physical environment, like temperature and pH. (samad et al,2015)

1.3.6 Electric double layer around dendrimers

A cloud of ions with high concentrations of counterions and low concentrations of coions surrounds a charged surface to form the electrical double layer. Usually, the EDL has a thickness of only a few nanometers.

Because of the many applications that are related to EDL features, such as colloidal stability, electrokinetics, the description of biological systems, and industrial products like inks, paint emulsions, food, or pharmaceuticals, an understanding of these properties is crucial for research and technology.

In the electrical double layer, oppositely charged particles attract to one another and have a tendency to cluster at the surface of each substance, but they are kept separate from one another by neutral molecules that surround the charged particles or by the limited size of each particle. The electrostatic attraction between opposing and separated charges produces an electrical field over the interface.

Dendrimers suspended in liquids are surrounded by oppositely charged ions. Their surrounding environment consists of two regions: the Stern layer, where the ions are firmly bound, and the diffuse outer region, where the ions are less closely bound. The diffuse outer region, which resembles a cloud of ions opposite in polarity, is held together by electrostatic forces. The entire system forms an electrical double layer; the formation of a net charge on the liquid surface of the bubble particle affects the distribution of ions in the nearby interface region, resulting in an increase in the concentration of counterions near the surface. Nano bubbles move along with the liquid as they pass through the boundary, but ions outside the boundary do not move along with it, and the boundary is referred to as the hydrodynamic shear force or the sliding plane, while the potential on this surface is called the zeta potential. (Kesharwani and Gupta, 2019)

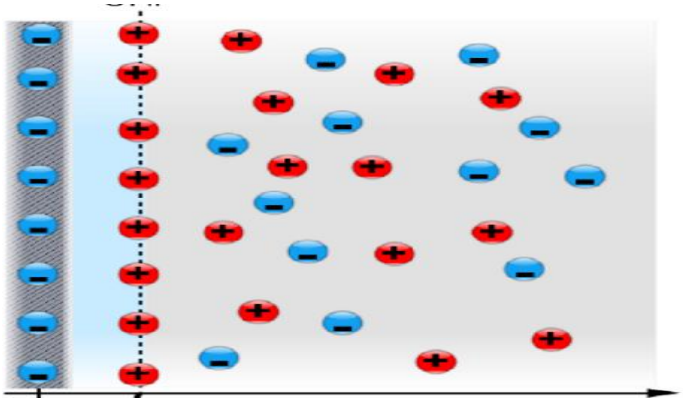

Figure 1.4: Schematic illustration of the Helmholtz EDL model.

1.4 Micelle

The term "polymeric micelles" refers to structured auto-assemblies made of amphiphilic macromolecules that develop in a liquid. In terms of structure and function, these self-assembled micelle structures mimic biological transport systems and can protect insoluble hydrophobic drugs. For a variety of various compounds, including low molecular mass hydrophobic drugs, proteins, and genes, micelles have been widely used as drug delivery systems. (Lu et al., 2018)

Micelles are made of surfactants (spherical structures with head surfaces that are hydrophilic on the outside and hydrophobic tails on the inside), and their size can vary between 10 and 100 nm; however, they can also be ellipsoid or cylindrical. Usually, the development of micelles is highly influenced by the specific characteristics of the electrolyte used. (Mahfuz et al., 2022).

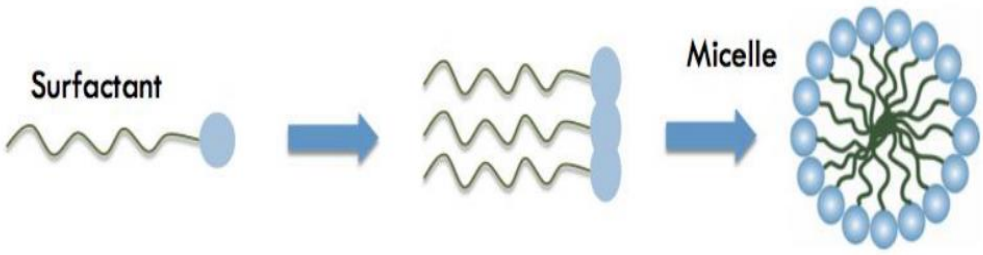

Figure 1.5: Micelles are self-assembled molecules made up of surfactants and lipids (molecules with hydrophilic heads and hydrophobic tails)

1.5 DLVO Theory

Derjaguin, Landau, Verwey and Overbeek developed the well-known DLVO theory in the 1940s (Derjaguin and Landau, 1941; Verwey and Overbeek 1948).

An attractive van der Waals interaction and a repellent electrostatic double layer interaction contribute to the DLVO interaction energy of a system of colloidal particles with like charges. Dispersions of colloidal particles typically have larger particle sizes and separation distances than the range of these interactions. The total potential energy of a particle in solution determines its stability in solution. (Derjaguin, 1993).

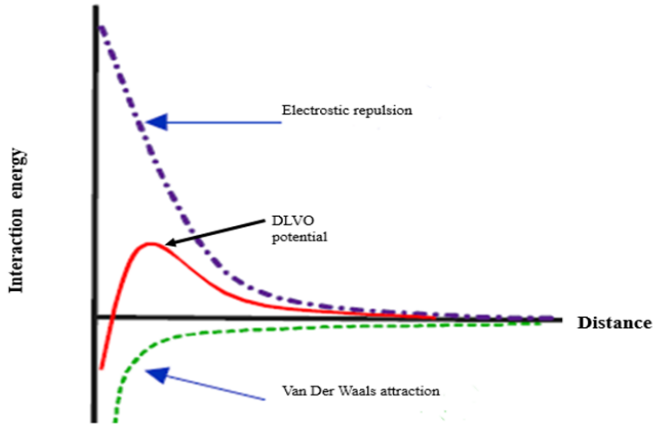

Figure 1.6: The continuous line represents the total of the two DLV interactions.

1.6 zeta potential

Zeta-potential, often denoted as ζ-potential, is the abbreviated term used to describe the electrokinetic potential in colloidal systems. It is a quantitative measurement of the force of electrostatic attraction or repulsion between nanoparticles, bubbles, or droplets. It is between the stern plane and the end of the diffuse layer. (Honary and Zahir, Part 1, 2013)

The main variables affecting the rate of drug desorption in nanoparticles and the effectiveness of drug loading are the surface charge of the particles and the kind of binding between the drug and nanoparticles. Moreover, the presence of a charged active substance within the center of the nanoparticle or only on its surface can be determined using the zeta potential, and the properties of a charged particle that is suspended in a liquid medium and surrounded by an electrical double layer depend on both the medium in which it is located and the particle itself. (Feng, Kilker and Lee, 2020)

The various features of nano-drug delivery systems are greatly affected by the zeta potential (ZP) of colloidal systems and nanomedicines as well as their particle size. ZP has a significant impact on dosage form stability and release rate, as well as on how well they circulate in the bloodstream and penetrate body membranes.

Zeta has been studied in several applications: in drug delivery systems, on the immunogenicity of nanoparticles, on pharmacokinetics and on tumor cell targeting. (Honary and Zahir, Part 2, 2013)

By using laser doppler velocimetry (LDV), zeta potential measurements are performed across an electrical field to determine the electrophoretic mobility of nanoparticles (Clogston and

Patri, 2011). It can be used to improve dispersion, emulsion, or suspension formulation by providing detailed insight into the causes of dispersion, aggregation, or flocculation of the particles. (Joly et al., 2004)

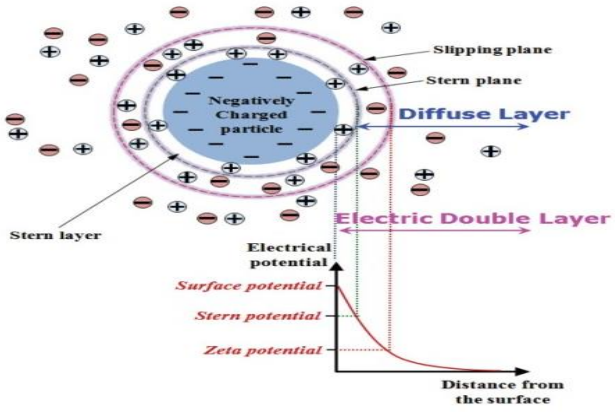

Figure 1.7: Schematic representation of zeta potential (ζ).

1.7 Charge inversion

Overcharging, or charge inversion, is a critical electrical phenomena, that is evident in biological molecular biophysics and colloidal systems. Electrostatic interactions in an electrolyte solution are screened by mobile ions. Strange phenomena like the attraction between ions with the same charge and the repulsion between ions with opposite charges can be observed in the presence of multivalent ions. (Besteman, Zevenbergen and Lemay, 2005).

It should be noted that when the screening occurred, the macroion's effective charge appeared to be smaller when observed from a limited point. Following that, the protected macroion's charge is observed from the outside as having the opposite sign. In order for the negatively charged DNA macroion to approach a negatively charged cell membrane, charge inversion is required. (Sinha *et al.*, 2017)

1.8 Previous studies

1. Joly, L., Ybert, C., Trizac, E., and Bocquet, L. (2004) studied the hydrodynamics within the electric double layer on slipping surfaces.The researchers demonstrate using extensive molecular dynamics simulations that the dynamics of the electric double layer (EDL) are strongly affected by the wettability of the charged surface where it develops. They showed that the dynamics of a wetting surface, characterized by the zeta potential, is controlled mainly by the electric properties of the surface, and they provide a clear explanation for the traditionally argued immobile Stern layer. For non-wetting surfaces, on the other hand, the immobile layer disappears. In addition, the electrokinetic zeta potential is greatly magnified by a slippage on the solid substrate.

2. Clogston, J. D., & Patri, A. K. (2011) studied Zeta potential measurement in the Characterization of nanoparticles intended for drug delivery. This article describes a method for measuring the electrostatic potential at the electrical double layer surrounding a nanoparticle in solution. The zeta potential is the result of this measurement. An estimated neutrality is generally considered to be achieved between nanoparticles of zeta potentials between *10 and +10 mV, while strongly cationic nanoparticles and strongly anionic nanoparticles with zeta potentials greater than +30 mV and less than −30 mV are considered strongly cationic and strongly anionic, respectively. Considering that most cellular membranes are negatively charged, a nanoparticle's zeta potential can influence its ability to penetrate membranes, with cationic particles displaying increased toxicity as a result of disrupting cell walls. It is shown that this technique can be applied to two types of nanoparticles that are commonly found in biological applications: colloidal gold (strongly anionic) and PAMAM dendrimers (strongly cationic).

3. Honary, S., and Zahir, F. (2013) studied the effect of zeta potential on the properties of nano-drug delivery systems-a review (Part 1). They studied a nano-drug delivery

system that has a variety of properties determined by the zeta potential, which is a term for electrokinetic potential in colloidal systems. Due to their exceptionally high potential for overcoming old challenges such as poor drug solubility and bioavailability, colloidal nano-carriers are growing rapidly today. In addition, they exhibit an unlimited ability to target drugs. A number of physical and chemical characteristics of nano-drugs have a significant effect on nano-medicine properties, including the release of nanomedicines at specific sites, circulation, and absorption into body membranes. Two key factors in this regard are particle size and charge.

4. Dias, A. P., da Silva Santos, S., da Silva, J. V., Parise-Filho, R., Ferreira, E. I., El Seoud, O., and Giarolla, J. (2020) studied dendrimers in the context of nanomedicine. A number of biological applications of dendrimers have been investigated, including delivery of drugs, DNA, RNA, and proteins, and imaging and contrast agents. This review provided examples of dendrimers used in nanomedicine in light of that. The majority of studies focus on cancer, yet there are studies showing that it also reduces neuroinflammation or protein aggregation in the nervous system. Dendrimers can deliver bioactive compounds by means of a covalent bond (dendrimer prodrug), ionic interaction, or adsorptive interactions with the internal space of the nanostructures. Moreover, dendrimers can be associated with polymers, such as polyethylene glycol, and with targeting agents such as aptamers, antibodies, folic acid, and carbohydrates.

5. Jiang, L., Zhou, S., Zhang, X., Wu, W., and Jiang, X. (2018) studied Dendrimer-based nanoparticles in cancer chemotherapy and gene therapy. The aim is to discuss the studies on dendrimer- based nanoparticles in cancer chemotherapy and gene therapy. A combination of dendrimers and specific tumor microenvironments is essential to deliver and control therapeutic agents to tumor tissues and cells with high efficacy and low side effects. Several strategies are presented in this review for designing the dendrimer-based delivery systems, including non-modified dendrimers, dendrimer conjugates, assembled amphiphilic dendrimers, nanohybrid dendrimers, and dendrimers with inherent activity. Further, functional groups are considered as stimuli-responsive delivery systems for targeting and controlling drug release. [25]

6. Zhao, H., and Bau, H. H. (2009) studied the polarization of a nanoparticle surrounded by a thick electric double layer. Using a standard model (the Poisson–Nernst–Planck PNP equations), they studied theoretically the polarization of a charged nanoparticle enclosed by a thick electric double layer and subjected to an alternating electric field. Calculating the dipole coefficient (f) requires knowing the electric field's frequency and the double layer's thickness (λD). They derived an approximately analytic expression for the dipole moment coefficient for a weakly charged particle with a small zeta potential ζ, which is accurate to within O (ζ2). As the thickness of the electric double layer increases, the importance of the particle's electrophoretic motion increases. The dipole moment is produced by two processes: ion transport in the electric double layer under the action of the electric field, and electron transport. The particle with the thick double layer has a higher level of dispersion than the particle with the thin double layer. Various theoretical predictions are compared to experimental data, and the results agree well, leading to the conclusion that the standard PNP model is an accurate representation of nanoparticle behavior under electric fields.

7. Kh.Qamhieh and V.Lobaskin (2003) studied the electrostatic principles of the instability of highly asymmetric electrolytes and utilized Monte Carlo simulation to explain the effective charge of the macroion and stability of asymmetric electrolyte solutions at various salt concentrations. They made use of a model containing charged macroions suspended in a multivalent salt solution. The findings indicate that the multivalent counterions' adsorption reduces the macroion's effective charge at low salt concentrations. But with high salt concentrations, the reversed charge rises as the macrions become overcharged.

8. Kh.Qamhieh, and coworkers (2013) used discrete spherical macroions charge distributions to examine the impact of the electrical double layer. The impact of substituting discrete macroions charge distributions for the traditional uniform macroions surface charge density on the properties of the electric double layer (EDL) in the solution was explained using Monte Carlo simulation. Two discrete models were used in addition to the core macroions charge: point charges constrained to the macroions' surfaces and finite-sized protrusion charges. The final results of calculating

the radial functions of charge densities and the potential of 10 electrical double layers were compared to those discovered for the charge distribution of the central macroions.

9. K. Qamhieh and P.lines (2005) used Monte Carlo simulations to examine the effects of switching from the typical uniform macroion surface charge density to discontinuous macroion charge distributions on the structural properties of aqueous solutions of like-charged macroions. They examined two discrete charge distributions: point charges on the macroion surface and finite-sized charges poking into the solution. They conducted tests using both fixed and mobile macroion charges, as well as discrete charge distributions. Point charges concentrated on the macroion surface cause counterions to grow larger when they are added to it, and the influence increases with counterion valence.

10. A.Zinchenko and N.Chen (2006) highlights the early stages of progress inspired by nanotechnology, which is concentrated on experimental physico-chemical and biophysical studies as well as theoretical and computational research on the compaction of DNA on nanoscale three-dimensional templates. Among the well-known examples of such a naturally occurring arrangement of a semi-flexible chain on nanoscale objects is DNA. Dendrimers, nanoparticles, and nanotubes are examples of various nanoscale three-dimensional structures that have been made possible by the rapid advancement of nanoscale chemistry and materials science. These structures have served as a foundation for the development of novel DNA-containing nanostructures, the modeling of natural DNA compaction, and the validation of accumulated theoretical predictions regarding the interaction between DNA and nanoscale templates.

11. S.Tripathy and M. Das (2013)clarify many dendrimer structural features and applications in medicine as prospective new drug delivery systems.As a nanocarrier, dendrimers are currently very sought-after for delivering medicinal compounds via various pathways. Regardless of several synthetic and regulatory limitations, dendrimers have the necessary qualities to position themselves as a possible carrier for the delivery of medicinal medicines.

    Dendrimers are the perfect building blocks for self-assembling and self-organizing systems because of their nanoscopic size and recognition capabilities. Hydrophobic and

hydrophilic medications can be adjusted to fit inside the dendritic structure's cavities. In addition to providing miscibility, reactivity, and solubility, the terminal groups are changed to attach antibodies and bioactive compounds for targeted purposes.

12. Per Linse and Leo Lue (2011) investigated models of charged spherical colloids in solutions free of salt, including situations where the inner dielectric constant of the macroions is lower than that of the surrounding solution. Utilizing a a novel, precise, and fast technique for quantitatively analyzing the electrostatic polarization interaction, simulations were carried out. The field theory predicts that counterion distributions outside of macroions will be in good agreement with simulation results across the whole range of electrostatic coupling from weak to solid, and a low-dielectric macroion will cause counterions to be driven away from the macroion systems. Hydrophobic and hydrophilic medicines may be incorporated into the dendritic structure's cavities by modification. Along with supplying miscibility, reactivity, and solubility, the terminal groups are changed to attach antibodies and bioactive compounds for targeting.

13. Mohammad Najlah and coworkers (2007),investigate in vitro, G0 PAMAM dendrimers were explored as drug carriers. Connecting naproxen directly via amide linkage to the G0 dendrimer resulted in highly stable prodrugs in plasma and liver homogenate. The use of a lactate ester linker produced prodrugs with high plasma stability and gradual hydrolysis in liver homogenate. Conversely, employing diethylene glycol as a linker yielded an ester conjugate displaying high chemical stability. Notably, attaching a lauroyl chain to the G0 PAMAM dendrimers' surface led to a more pronounced increase in naproxen transport. These findings suggest the potential of G0 PAMAM dendrimers as nanocarriers for enhancing oral bioavailability.

14. Domenico Marson and coworkers(2019) part one, they Designed, synthesized, and tested highly flexible triethanolamine-core PAMAM dendrimers proved to be a successful approach for siRNA delivery in cancer therapeutics. The G5 TEA-core PAMAM dendrimer demonstrated remarkable effectiveness, leading to its scheduled entry into clinical trials for siRNA-based cancer therapy. Additionally, amphiphilic dendrons, capable of auto-organization into micelles, mimicked covalent, high-generation dendrimers in size, structure, and function, particularly excelling in siRNA delivery.

15. Domenico Marson and coworkers(2019) part two,The investigation focused on a small PAMAM-based amphiphilic dendron, denoted as 4, featuring a PAMAM head and a C18-long hydrocarbon tail. This dendron demonstrated safety and efficacy in delivering siRNA, both in vitro and in vivo. Its evolution led to the development of the double-tail counterpart,

AD, which exhibited a comparable in vivo gene silencing effect in cancer treatment to its precursor dendron 4. Notably, AD nanovectors displayed the ability to induce gene silencing effects in challenging and treatment-refractory human primary cells and stem cells. The RNAi outcomes for both amphiphilic dendrons 4 and AD were primarily attributed to passive targeting via the EPR effect, coupled with their capabilities.

1.9 Statement of the problem

In our study, we used Monte Carlo simulation to find the zeta potential of an electric double layer for dendrimers. This simulation study has an important practical significance and is an exciting area for more research in gene therapy. It can give us predictions about the appropriate structure of the dendrimer with high efficiency in order to reach the target in a specific environment.

This simulated work has studied the effect of different radius of macroions according to the radial distribution function and the potential for different generations in an aqueous solution with a certain dielectric constant without salt. We also compared the effect of changing the radius of the sphere in a hard spherical model.

In addition, we investigated the results of the dendrimers in a solvent with a dielectric constant that represents the cytoplasm. In this case, the macroions and counterions electrostatically interacted. We compared our findings with the results of previous simulations.

Chapter Two

Model and method

2.1 Introduction

Monte Carlo (MC) simulation has been used to achieve the goal of this study. Primarily to examine the colloidal particle's response to the macroion dielectric constant, and the effect on the properties of the EDL was recorded. (Raychaudhuri, 2008)

A type of simulation known as a Monte Carlo simulation uses statistical analysis and repeated random sampling to determine the outcomes. This simulation technique is similar to random experiments, in which the specific results are undefined. (Liu,2004).

Monte Carlo methods are used in a variety of fields, including biology, chemistry, economics, finance, engineering, material science, and others.

Monte Carlo simulation is a powerful technique for tackling complex physical problems due to its ability to handle a large number of random variables, various distribution forms, and especially non-linear engineering models. (Siddall,1983)

Asymmetric electrolytes are the system under consideration, which are characterized using the primitive model. There are macroions and counterions in the system.

2.2Model:

The solvent is treated as a dielectric medium without salt, and we built our model by using a hard sphere to represent a macroion. The soft sphere is considered a dendrimer of radius **R**. Counterions, depicted as small, rigid spheres with varying sizes and carrying a charge of (**ZIe = +1e**), are part of a system in a solvent treated as a dielectric medium without salt. These counterions play a crucial role in electrostatic interactions within the medium, contributing to the overall behavior and dynamics of the system.

Macroion models can be established by varying the radius ($\mathbf{R_m}$) and charge (**Z**) of the macroions, with e representing the elementary charge. This approach enables a comprehensive investigation of the system's behavior, as long as proper citations and references are provided.

The counterions are depicted as charged hard spheres with a specific radius **R1** and charge **Z1**. The entry of water into the system is influenced by its relative dielectric permeability (see Figure 1).

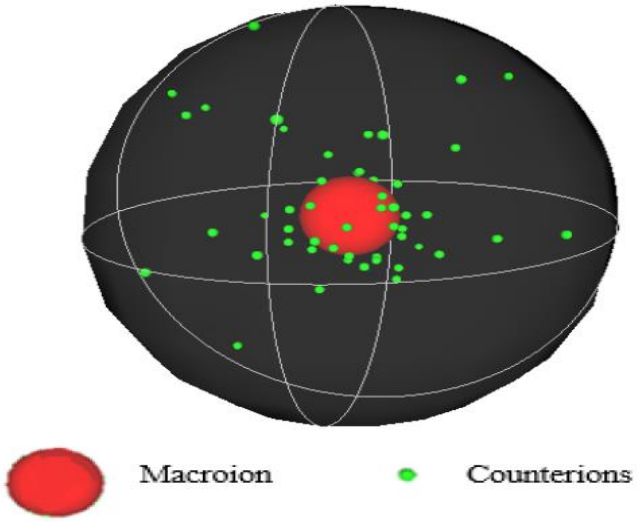

Figure 2.1: Cell boundaries have a spherical shape. The macroion is depicted as a red sphere, while the counterions are represented by smaller green spheres.

The system's total potential interaction energy U, is defined as:

{U = U_{HS} + U_{Elec} + U_{Ext}} Eq 2.1

- **U_{HS}** refers to the Hard-sphere repulsion.
- **U_{Elec}** denotes the Coulomb interaction.
- **U_{ext}** represents the confinement potential energy. (Nguyen et al,2000)

➢ Hard-spher repulsion which is given by:

$$U_{hs} = \sum_{I<j} \bigcup_{Ij}^{hs}(r_j) \quad Eq.2.2$$

with

$$\bigcup_{Ij}^{hs}(r_j) = \begin{cases} \infty, & r_j < R_I + R_j \\ O, & r_j \geq R_I + R_j \end{cases} \quad Eq.2.3$$

Where Ri denoting the radius of the particle (i and j denote either a macroion, a macroion location, a macroion positions or a counterion) and rij is the distance between the centers of particles i and j.

- The Coulomb interaction:

$$U_{elec} = \sum_{I<j} \bigcup_{Ij}^{elec}(r_j) \quad Eq.2.4$$

With

$$\bigcup_{Ij}^{elec}(r_j) = \frac{z_i z_j e^2}{4\pi\varepsilon_0\varepsilon_r r_{\mathrm{Ij}}}, \quad Eq.2.5$$

A particle i can be either a macroion or a counterion, and its charge is implied by Zie; the elementary charge is represent by e, while the permittivity of vacuum and relative permittivity of the solvent are denoted by ε0 and εr, respectively.

- The confinement potential energy:

$$U_{ext} = \sum_{\mathbf{I}} \bigcup^{ext}(r_I) \quad Eq.2.6$$

With

$$\bigcup^{ext}(r_I) = \begin{cases} 0, & r_I \leq R_{sph} \\ \infty, & r_I > R_{sph} \end{cases} \quad Eq.2.7$$

Where R_{sph} represents the radius of the spherical cell.

We'll use models that were resolved by running the computerized programs utilizing the Monte Carlo (MC) simulation method, based on the calculations required for the simulation task.
This approach, which is derived from the conventional Metropolis algorithm with certain modifications, will be utilized for simulating multi-particle systems within the canonical NVT ensemble (where particle number, volume, and temperature are held constant). (Lobaskin and Qamhieh, 2003).

The assessment of potential energies was carried out by applying equations (2.3)-(2.7). Consequently, For a spherical cell, each interaction will be dealt with, the potential cutoff will be set and the long-range Coulomb interaction will be handled using Ewald summations. (Qamhieh and Linse,2005).

Firstly, to crat an initial configuration, the macroion will be positioned at the center of the spherical cell. The counterions from G1 to G6 were positioned randomly 10^6(steps/ passes) and G7 to G8 were 10^5 (steps/ passes) moves per particle before equilibrating (production) and also after equilibrating to reach the stability of energy.

In this particular model, it is assumed that we have a system of solutions consisting of asymmetric electrolytes, which are composed of two distinct categories of charged spherical particles known as macroions and counterions. The macroion is represented as a rigid sphere with a radius of ($\boldsymbol{R_M}$) and a specific charge ($\boldsymbol{Z_M e}$), and 'e' denotes the elementary charge. The counterions are depicted to be smaller with a radius of ($\boldsymbol{R_I = 2A}$) and a charge of ($\boldsymbol{Z_I e}$=**-1e**), considered within the confines of the fundamental model, wherein the solvent is incorporated into our model through its dielectric constant. In our study we used two solvents, the first one is water with dielectric constant (ε_r = 78.4), and another solvent with a dielectric constant (ε_r = 10) represents the cytoplasm of the cell. The temperature was kept constant at, T=298 K.

Two free salt systems are discussed in this work:

1- Radius of sphere is constant (R_{sph}=100), macroion number density is constant

For this system that is represented in table 2.1 and 2.1 we demonstrated Z_M=charge of macroion and R_M=Radius of macroion for each generation. In table 2.1 we calculated volume fraction of the macroion ($\emptyset_M$).

$\emptyset_M = \frac{Macroion\ volume}{Spherical\ cell\ volume} = \frac{V_M}{V_c} = \frac{\frac{4}{3}\pi R_M^3}{\frac{4}{3}\pi R_C^3} = \frac{R_M^3}{R_C^3} = \left(\frac{R_M}{R_C}\right)^3$, where R_M=Radius of macroion, R_{sph}= Radius of sphere= 100 ,With a constant macroion number density $\rho_M = 2.5 * 10^{-7}\ A^{-3}$

Table2.1: shows the specification of each generation when R is constant.

Generations	G1	G2	G3	G4	G5	G6	G7	G8
Charge(Z_M)	8	16	32	64	128	256	512	1024
Radius Å (R_M)	11	14.5	18	22.5	27	33.5	40.5	48.5
$\emptyset_M$	0.11	0.145	0.18	0.225	0.27	0.335	0.405	0.485

2- Radius of sphere is variable, macroion volume fraction $\emptyset_M$ is constant

For this system that is represented in table 2.2, we calculated the macroion number density(ρ_M)

$\rho_M = \frac{N_M}{Volume\ of\ the\ spherical\ cell} = \frac{N_M}{\frac{4}{3}\pi R_M^3} = \frac{1}{\frac{4}{3}\pi (Rc^3)}$ N_M= number of macroions.

, also we calculated the radius of sphere for each generation $R_{sph} = \left(\frac{R_M}{\emptyset_M}\right)^{\frac{1}{3}}$, this corresponds to the volume fraction of the macroion $\emptyset_M = 0.008$

Table2.2: shows the specification of each generation when R_{sph} is variable.

Generations	G1	G2	G3	G4	G5	G6	G7	G8
Charge(Z_M)	8	16	32	64	128	256	512	1024
Radius Å (R_M)	11	14.5	18	22.5	27	33.5	40.5	48.5
R_{sph} Å	55	72.5	90	112.5	135	167.5	202.5	242.5
ρ_M	$0.14*10^{-5}$	$0.063*10^{-5}$	$0.033*10^{-5}$	$0.016*10^{-5}$	$0.0097*10^{-5}$	$0.005*10^{-5}$	$0.0028*10^{-5}$	$0.0016*10^{-5}$

2.3 Method and Simulation setting:

The Monaco town of Monte Carlo, which is well-known for gambling, is the inspiration for the Monte Carlo simulation. In a mechanism where random variables exist, Monte Carlo simulations are used to model the possibility of multiple outcomes. It is a strategy for thinking about how uncertainty affect prediction models.

Monte Carlo is capable of handling huge numbers of random variables, multiple distribution forms, and engineering models that are mostly nonlinear, and it is very well suited for dealing with complex physical difficulties. (Siddall, 2003).

A summation of Ewald's equations will be used to deal with electrostatic interactions and the trial displacement method will also be used in various forms. Equations 1 to 7 that mentioned in the model section, were used to evaluate the potential energies in spherical cell conditions. The potential cutoff will be used, and all interactions have been considered. Finally, the

integrated Monte Carlo simulation tool has been used to conduct all the simulations (MOLSIM). (Per Lines et al., 2004). (For details, see the ref (Lines, 2015))

2.4 Metropolis Algorithm:

In 1953, Metropolis published a paper describing a method that became a key component of today's simulated annealing technology. Creating Boltzmann distribution samples from liquid numerical simulations was demonstrated in this paper.

Defining the range of input values that can be used to produce a lot of random configurations of the system, repeating the process numerous times (As additional runs are performed, the accuracy of the results improves) This algorithm uses the following arithmetic operations to calculate each configuration's properties (such as energy or density):

1. Select the particles to be moved randomly, then move them at a random distance.
2. The energy difference between the old and new configurations is equal to ΔU trial = U new - U old.

If ΔU trial is equal to or less than zero, then accept the new configuration; if not, don't accept the move and take the previous configuration as the new one. Finally, if the random number generator for $0 \leq x < 1$ is less than exp (-ΔU trial /KBT). A new trial move is attempted only once data for averages has been gathered after each step. (Schneider, 2003).

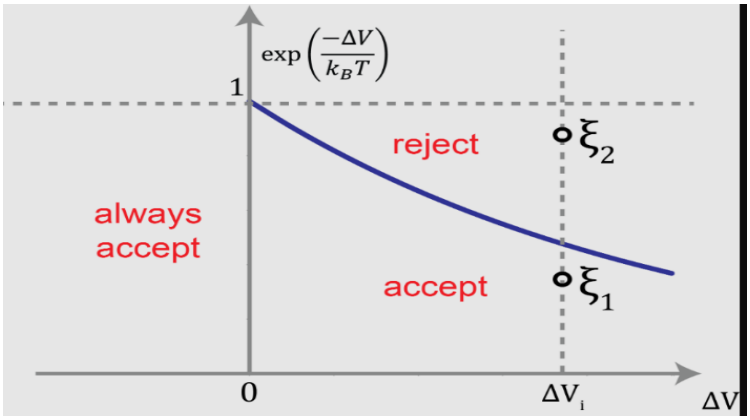

Figure 2.2: The Metropolis algorithm's scheme for accepting and rejecting trial motions.

Chapter three

Results and discussions

Chapter three

The results and outcomes are calculated and presented by an advanced computational software.

3.1 systems with water

A. Macroion number density is constant (R_{sph} is constant =100 A): radial distribution functions (RDFs) for counterions in a salt-free system in terms of the distance to the dendrimer's center (r). As shown in Figure 3.1

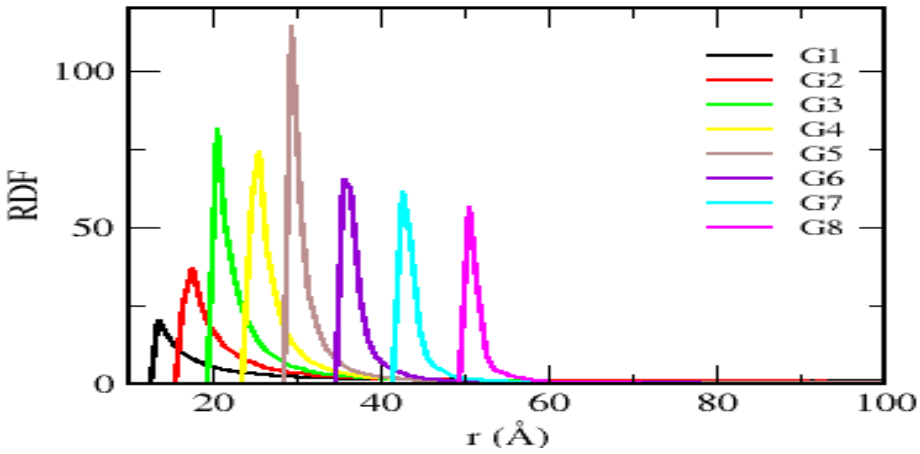

Figure 3.1: Dendrimers in G1 to G8 show radial distributions between macroions and counterions in relation to the distance (r) from their centers.

Figure 3.1 Shows the radial distribution function (RDFs) based on distance (r) from the dendrimer's center.

At a distance r from the dendrimer, RDFs indicate the relative density of a small, random distribution of the counterions. The values are set to unity when there is no spatial correlation between different generations., however, the maximum distribution in G5 shows the greatest electrostatic correlation.

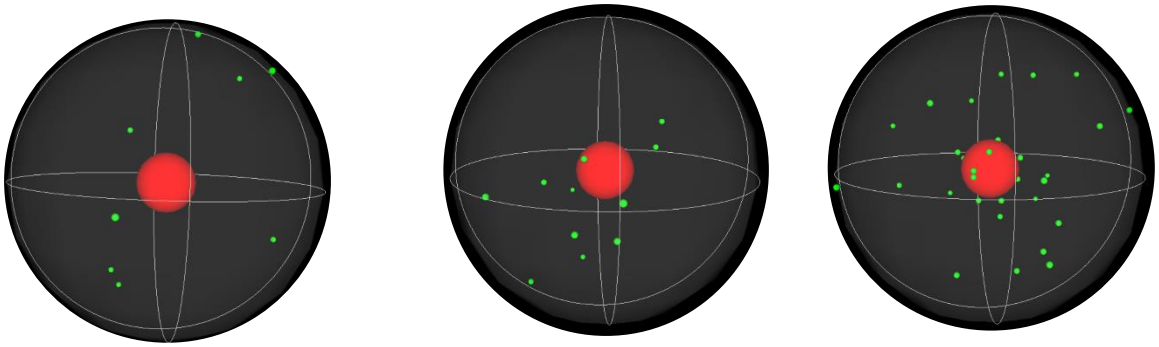

(a) (b) (c)

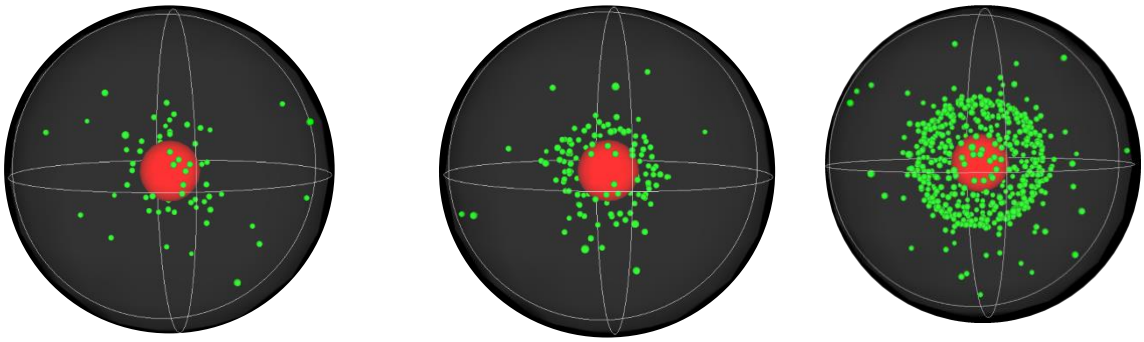

(d) (e) (f)

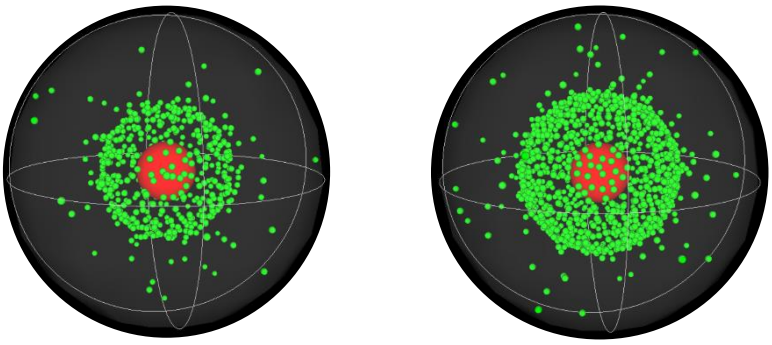

(g) (h)

Figure 3.2: The arrangement of the counterions, represented as small green balls, are organized around the dendrimers, which are large red balls. This arrangement occurs within a spherical space with a radius of 100 Å in water at macroion dielectric constant = 78.4: a) G1, b) G2, c) G3 d) G4, e) G5, f) G6, g) G7 and h) G8.

Figure 3.2 demonstrates the snapshots of the counterion distribution for each dendrimer's surface inside the spherical cell. It is evident that as generation increases, counterions accumulate closer to the macroion surface.

Equation 1 is applied to determine the Running Coordination Number (RCN), which represents the number of ions within the distance r from the macroion.

$$rcn\,(r) = \int_{r}^{\infty} \sum [Z_i * N_i / \left(\frac{4}{3}\right) * 3.14 * 100^3 Å3.* g_{Mi}] 4\pi r`^2 dr` \quad eq.1$$

Where the valence of counterions are represented by Z_i while N_i stands for the charge of the macroion, g_{Mi} refers to the RDF of the counterions around the macroion and the distance r` is measured from the dendrimer's center.

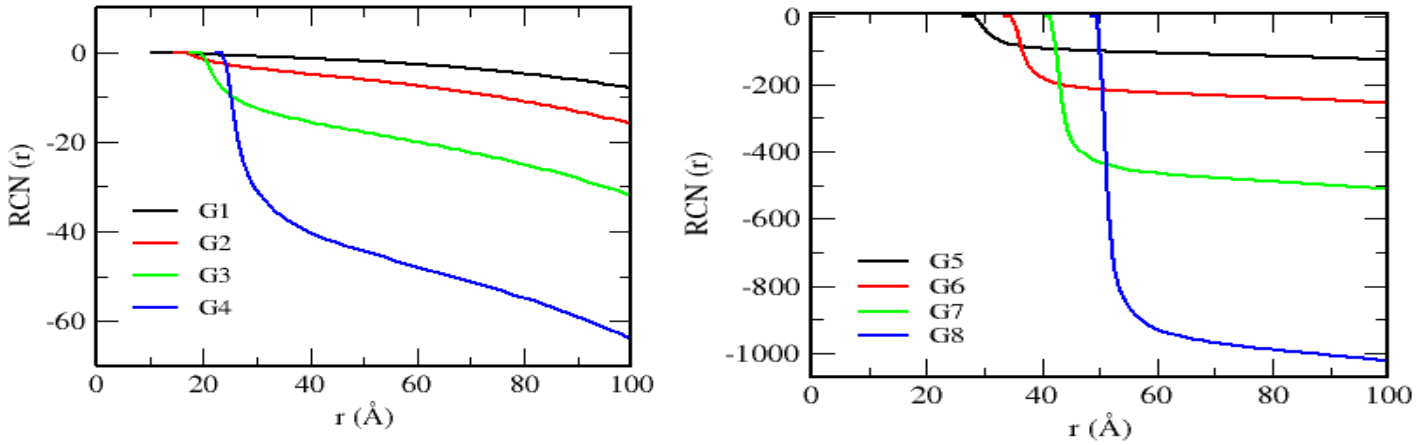

(a) (b)

Figure 3.3: (a) and (b) are the RCN (r) as a function of the distance r from the dendrimer for different generations.

In figure 3.3, we notice that the number of counterions increases as generations increase, as does the electrostatic correlation increase.

0Equation 2 is applied to calculate the accumulated running charge P(r) for a dendrimer when viewed from its center (r).

$$P(r) = Z_M + \int_r^{\infty} \sum [Z_i \rho_i(r`)] 4\pi r`^2 dr` \qquad eq.2$$

Where Z_M is used to represent the charge of the dendrimer, while Z_i stands for the valence of the counterions. Additionally, ρ_i signifies the uniform charge density of the counterions, and r` denotes the distance measered from the center of the dendrimer.

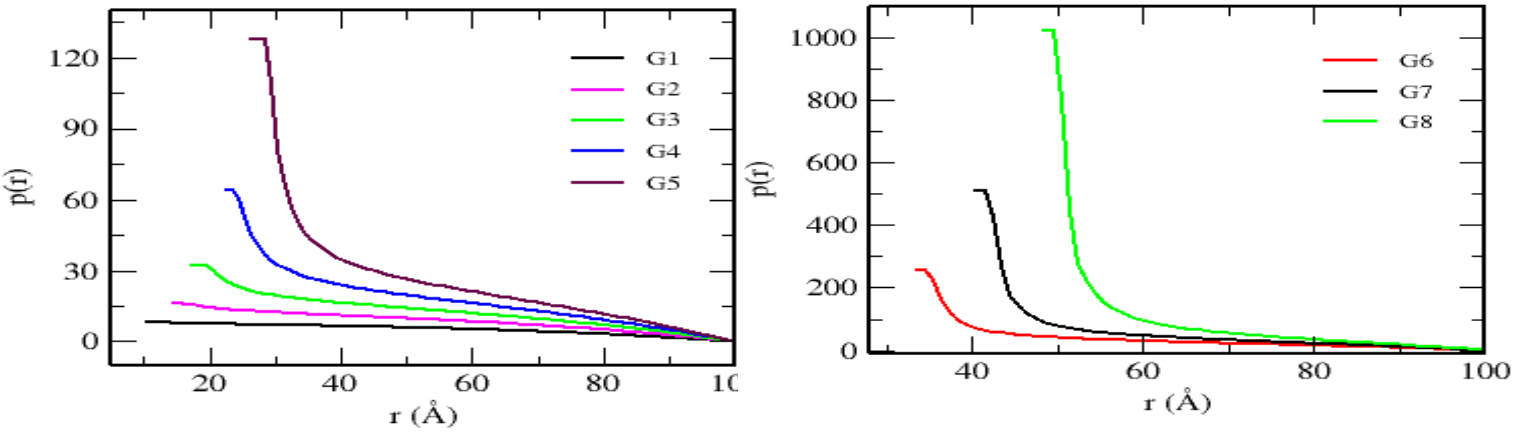

(a) (b)

Figure 3.4: (a) and (b) represents the integrated charge numbers denoted as P(r) within varying distances r from the dendrimer's center for different generation.

Figure 3.4 reveals a notable accumulation of the counterions near the dendrimer's surface, which intensifies as the dendrimer generation increases. Additionally, the figure illustrates that the attractive electrostatic interaction between the dendrimer and the counterions becomes stronger as the distance (r) from the dendrimer's center increases within the spherical cell.

The electrostatic potential (φ) of the Electric Double Layer (EDL) has been graphed for each generation, with respect to the distance (r) from the dendrimer's center, using equation 3:

$$\varphi(\mathrm{r}) = \frac{e}{4\pi\varepsilon`} \int_r^{\infty} dr` \frac{P(r')}{r`^2} \qquad eq.3$$

The elementary charge is often denoted as (e), a fundamental unit of electric charge, and P(r) is expressed as the integrated charge number within the distance (r`) from the dendrimer's center. Moreover, the permittivity of the solvent, is often represented as (ε`).

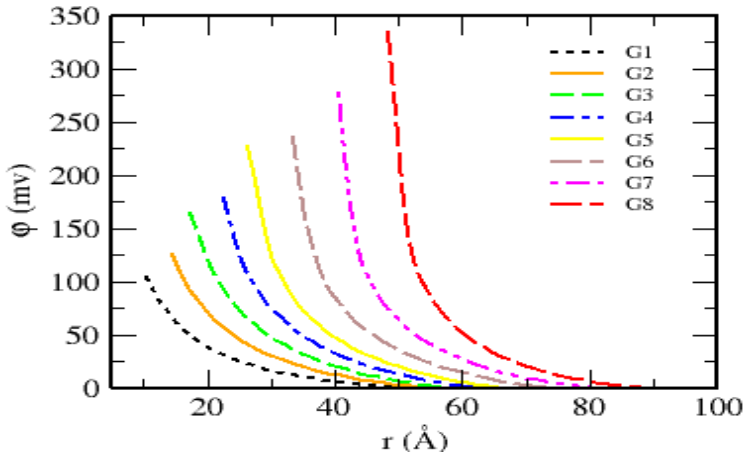

Figure 3.5: The electrostatic potential of the electric double layer represented as φ(r), within the distance from the center of the dendrimer.

.

Figure 3.5: Shows the electrostatic potential φ (r) of the electric double layer, we assume the zero potential at R_M+ 40 for each generation.

The magnitude of the electrostatic potential notably increases around the surface of the dendrimer, indicating a strong electrostatic influence in this region. This increase in electrostatic potential is correlated with the greater presence of counterions, suggesting that a higher concentration of counterions intensifies the electrostatic interactions with the dendrimer.

When there is an increase in counterion concentration at the surface, it leads to the formation of the electric double layer (EDL) around each particle. The distribution of ions within this interlayer has a notable impact on the development of a net charge. Zeta potential plays a significant role in this context because it serves as a crucial parameter. It can be correlated with the stability of colloidal dispersions. By understanding and controlling the zeta potential.

The zeta potential, illustrated in Figure 1.7 within the Electric Double Layer (EDL), signifies the potential of the slipping plane. It represents the difference in electrical potential between the bulk medium and the fixed layer of the liquid that surrounds the dispersed particles.

Figure 3.6 (a) shows the zeta potential (ζ), the values of the zeta potential increase by increasing the generation of the dendrimer, where the change becomes slower for generation from G5 to G8, and G8 values at the highest level achieve the maximum potential. Figure 3.6 (b) observed that the values of surface electrostatic potential (φs) on the surface of the dendrimers were found to be greater than the zeta potentials. And the surface of G8 dendrimers exhibited a higher electrostatic potential, and the values of the surface potential increased as the generation of the dendrimer increased.

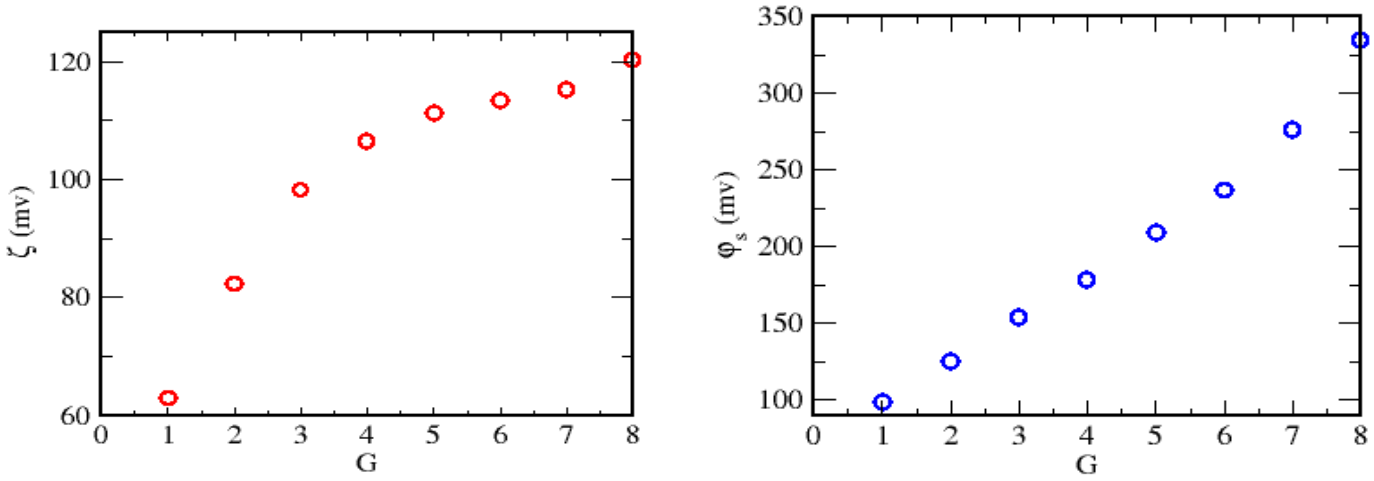

(a) (b)

Figure 3.6: (a) Zeta potential and (b) surface potential of the dendrimer.

From Figure 3.6, we calculated the zeta potential when r = R_M+4. It is obvious that when generation increases, the zeta potential's values increase linearly.

B. Macroion volume fraction $\emptyset_M$ is constant (R_c is variable) radial distribution functions (RDFs) for counterions in a salt-free system in terms of the distance to the dendrimer's center (r). As shown in Figure 3.7.

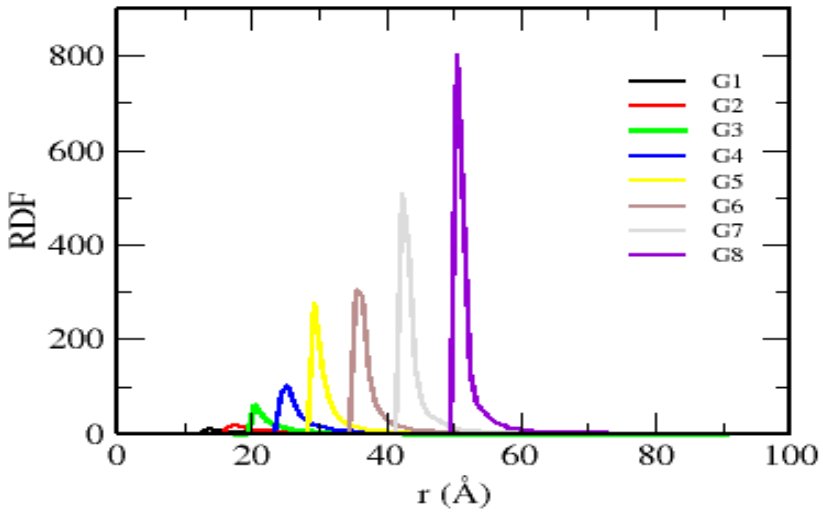

Figure 3.7: Dendrimers in G1 to G8 show radial distributions between macroions and counterions in relation to the distance (r) from their centers.

Figure 3.7 shows the density of small counterions at various distances (r) from the dendrimer within the spherical cell is depicted, and there is no spatial correlation. However, as demonstrated in the Figure, the distribution of counterions around the dendrimer intensifies with the increase in dendrimer generation. This observation suggests that higher dendrimer generations lead to a more pronounced accumulation of counterions.

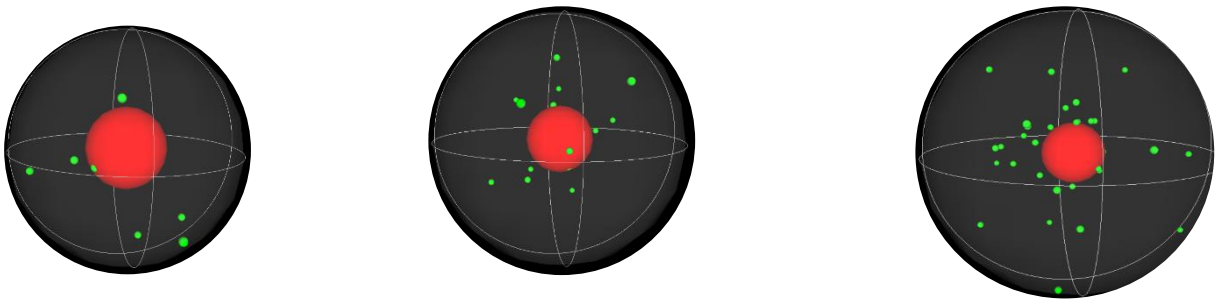

(a) (b) (c)

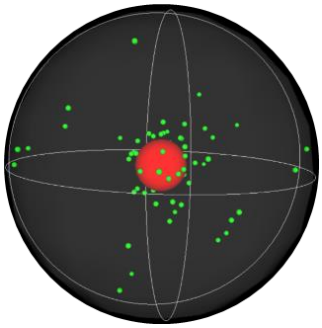

(d)

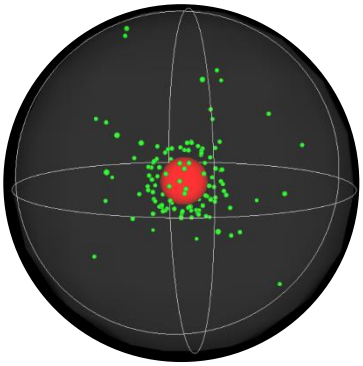

(e)

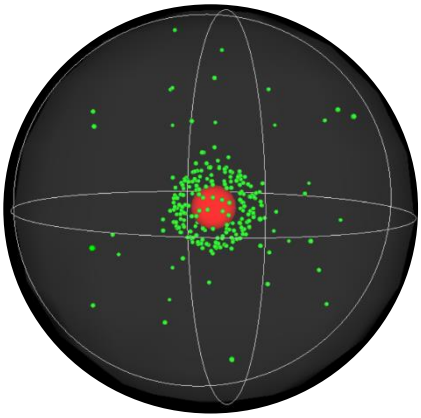

(f)

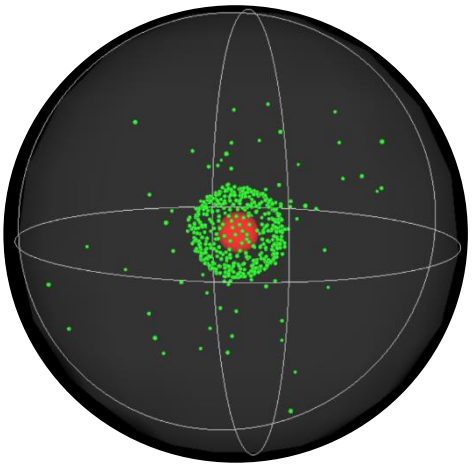

(g)

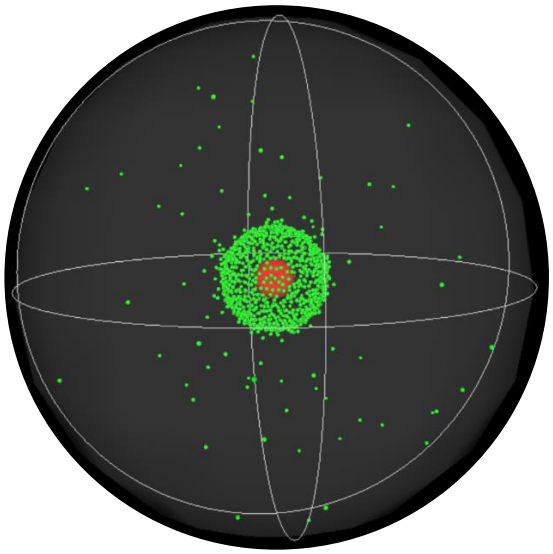

(h)

Figure 3.8: : The arrangement of the counterions, represented as small green balls, are organized around the dendrimers, which are large red balls. This arrangement occurs within a spherical space: a) G1, b) G2, c) G3, d) G4, e) G5, f) G6, g) G7, and h) G8.

According to Figure 3.8: The snapshots show the counterion distribution. Clearly, Rc increases and the counterions accumulate near the dendrimer's surface as well. This observation suggests that higher dendrimer generations lead to a more pronounced clustering of counterions around the surface.

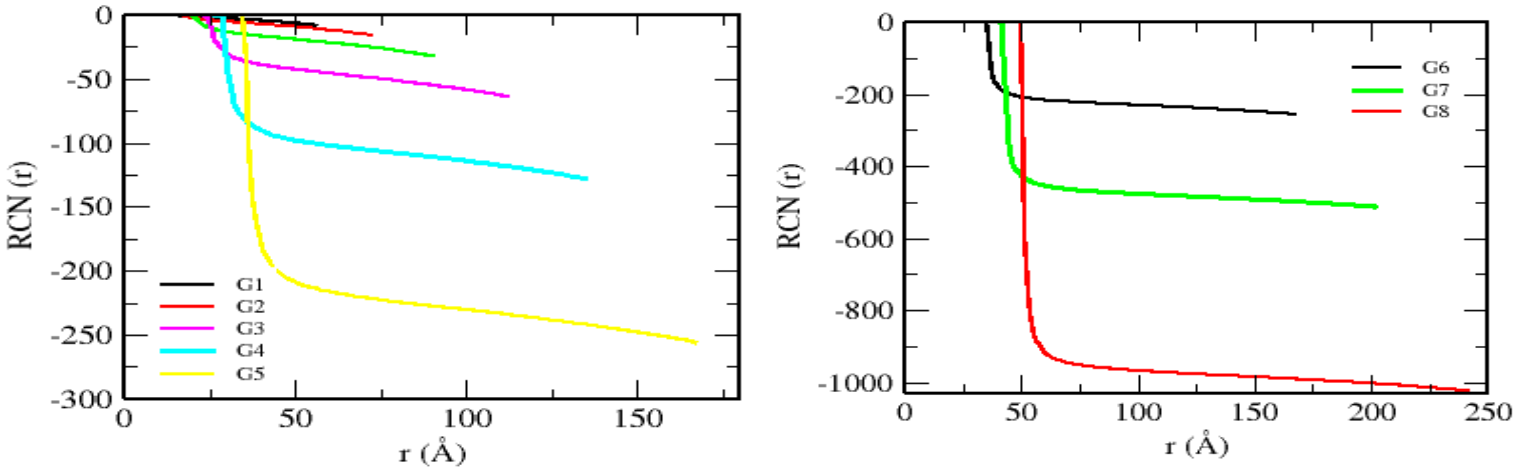

(a) (b)

Figure 3.9: (a) and (b): RCN (r) for different generations versus distance r from the dendrimer's center.

According to the figure 3.9 we note that the number of counterions increases when generation increase also the electrostatic correlation increase.

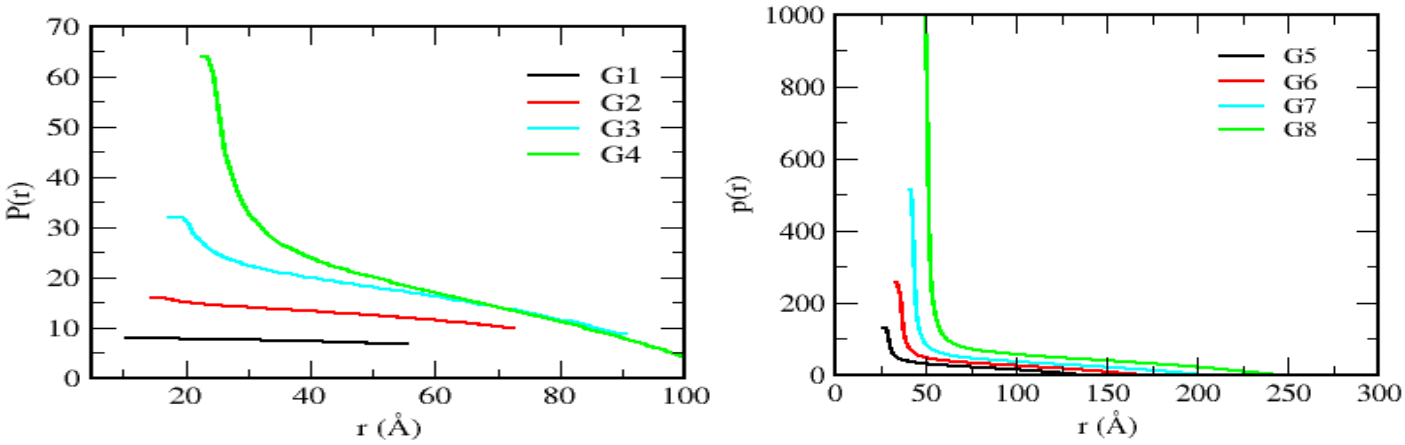

(a) (b)

Figure 3.10: (a) and (b): the integrated charge number P(r) for various generations inside the distance r from the dendrimer's center.

The data presented in Figure 3.10 indicates a clear trend where the accumulation of counterions around the dendrimer's surface becomes more pronounced as the generation of the dendrimer increases. Additionally, it suggests that the attractive electrostatic interaction between the dendrimer and the counterions becomes stronger as the distance 'r' inside the spherical cell increases. This phenomenon is likely due to the increased charge density as dendrimer generation grows.

The electrostatic potential φ(r) of the EDL for each generation has been plotted as shown in figure 3.11:

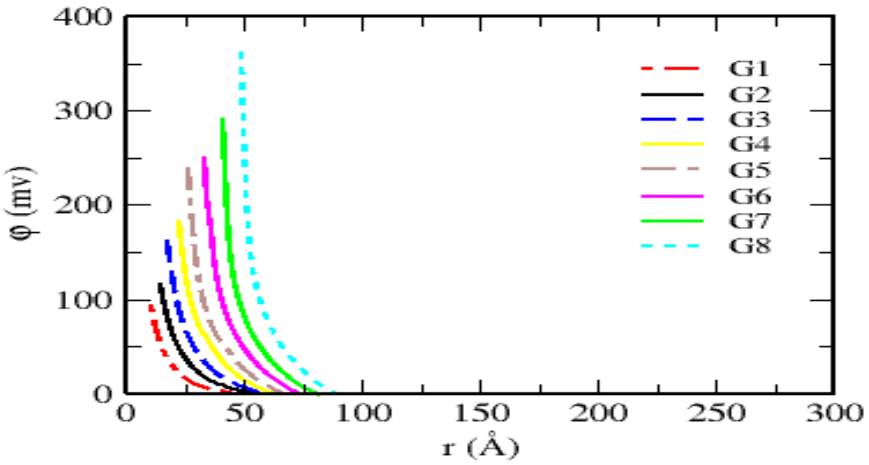

Figure 3.11: The electrostatic potential of the electric double layer represented as φ(r), within the distance from the center of the dendrimer.

Figure 3.11, shows the magnitude of the electrostatic potential increases near the surface of the dendrimer; it increases with the increase of the counterions, the electrostatic potential is increased as a result of increasing the electrostatic interaction between the dendrimer and the counterions; it also increases near the surface of the macroion by increasing the radius of the dendrimer.

Figure 3.12 (a) shows the zeta potential (ζ), the values of the zeta potential increase by increasing the generation of the dendrimer, where the change becomes slower for generation from G5 to G8, and G8 values at the highest level achieve the maximum potential. Figure 3.12 (b) (b) observed that the values of surface electrostatic potential (φs) on the surface of the dendrimers were found to be greater than the zeta potentials. And the surface of G8 dendrimers exhibited a higher electrostatic potential, and the values of the surface potential increased as the generation of the dendrimer increased.

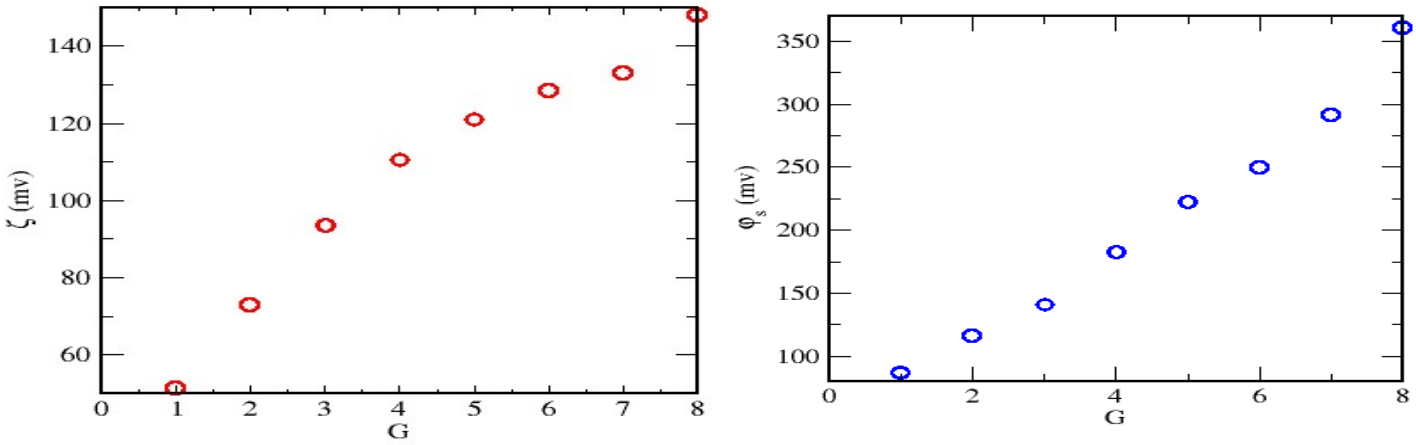

(a) (b)

Figure 3.12: (a) Zeta potential and (b) surface potential of the dendrimer.

From Figure 3.12, we calculated the zeta potential when r = R_M+4. It is observed that the zeta potential values within the interfacial double layer show a clear increase with each successive dendrimer generation.

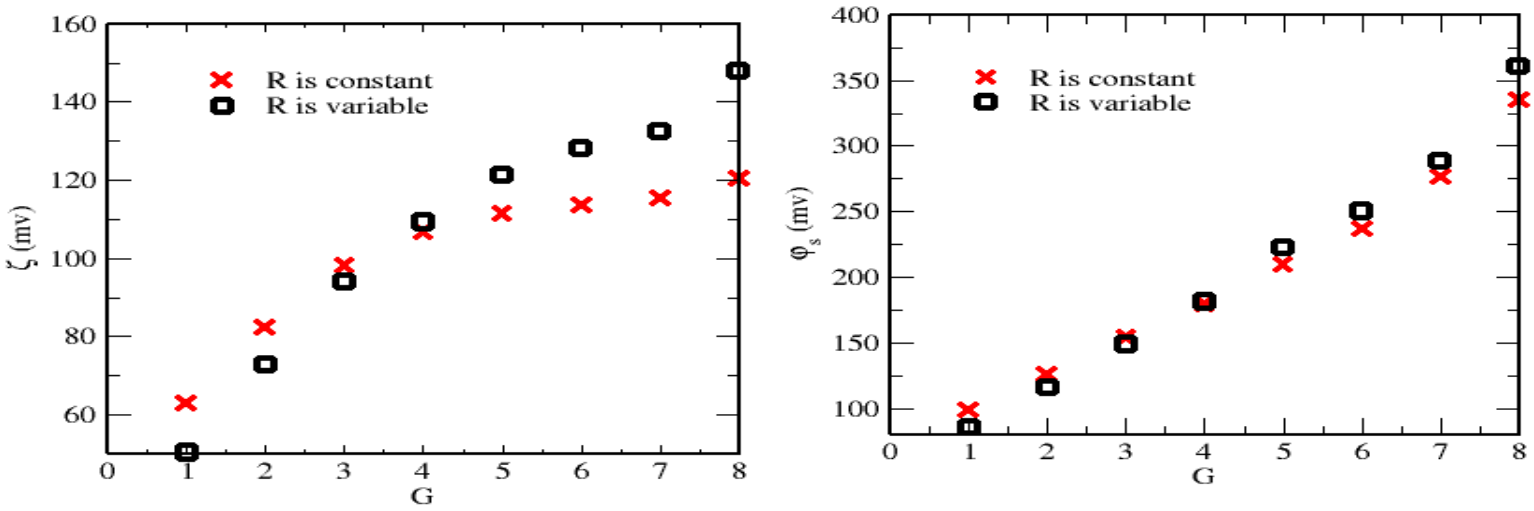

(a) (b)

Figure 3.13: (a) Zeta potential and (b) potential's surface of the dendrimer.

Generally, from figure 3.13, we notice that when the generation increases, the number of counterions increases. The values of zeta and surface potential increase, and electrostatic

potential increases. The greater the number of generations, the greater the ability of the dendrimer to attract counterions towards it because of the increase in the effective charge.

.

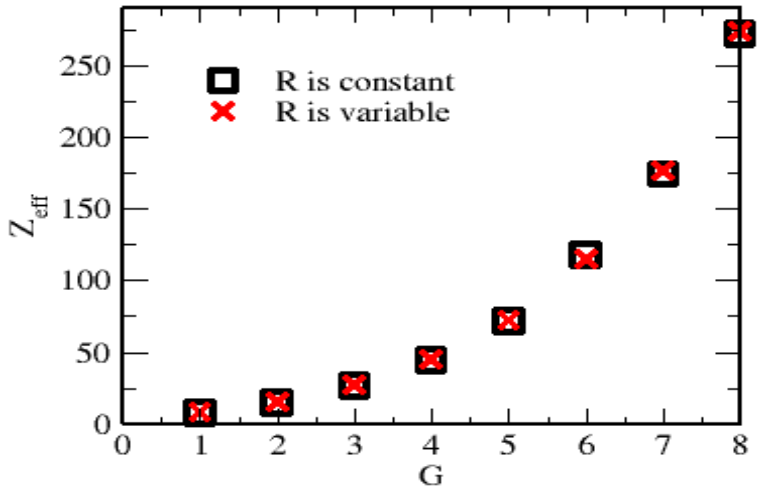

Figure 3.14: The ratio of effective dendrimer charge Z_{eff}.

Figure 3.14 shows the effective charge (Z_{eff}) at the distance R_M+4Å from the center of the dendrimer. The values are almost equal for R variable and R constant, and the effective charge (Zeff) increase in the positive region. That means the charge accumulation is high in both cases.

3.2 Dendrimers in solvent with dielectric constant 10 represents the cytoplasm.

Changes in the solvent's dielectric constant affect the behavior of the electrostatic interaction between the dendrimer and the counterions in the spherical cell model. In this case of a solution without salt, the dielectric constant is 10, which represents the cytoplasm. Therefore the counterions accumulated near the dendrimer surface, which was significantly impacted by the small dielectric constant, while the largest distribution occurred at the smallest generation as the interaction between the dendrimer and the counterions increased. As shown in figure 3.15:

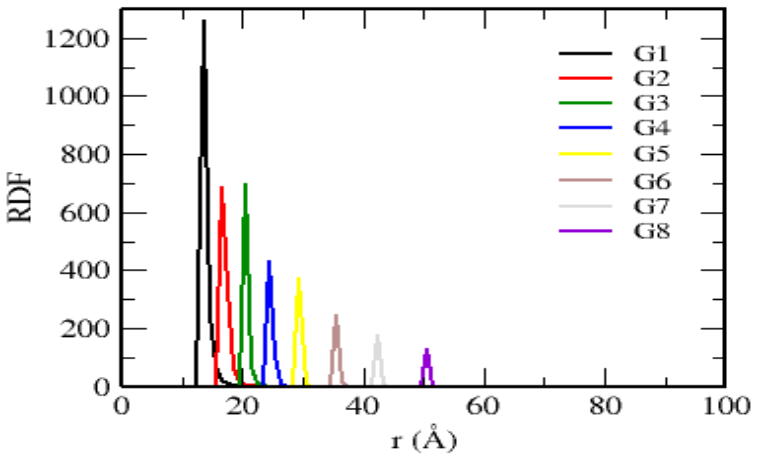

Figure3.15: Dendrimers in G1 to G8 show radial distributions between macroions and counterions in relation to the distance (r) from their centers.

Figure 3.15 illustrates the Macroion-Counterion Radial Distribution Function at a specific dielectric constant value of ε = 10. The dielectric constant, denoted as ε, is directly related to the Coulomb's law constant, K, as per the equation $K = 14\pi\varepsilon$. Therefore, as the dielectric constant ε decreases, it results in an increase in Coulomb's law constant K, which, in turn, affects the electrostatic interactions between the macroion and counterions in the system. This change in K influences the relative density of counterions at different distances from the dendrimer's center.

The charge distribution on the dendrimer's surface becomes more concentrated as the dendrimer's r decreases. This concentration of charge is most pronounced at Generation 1 (G1) and decreases gradually with higher generations, reaching its lowest value at Generation 8 (G8). Furthermore, as Coulomb's law constant (K) increases, there is a greater accumulation of charge near the dendrimer surface, especially at smaller dendrimer generations. These observations highlight the significant impact of generation size and the value of K on the charge distribution in the system.

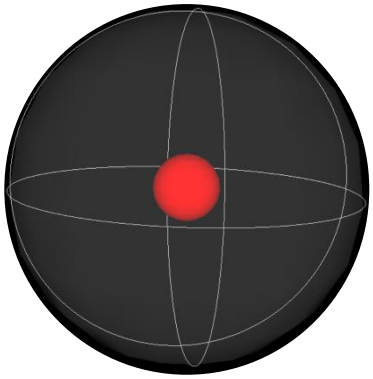

(a)

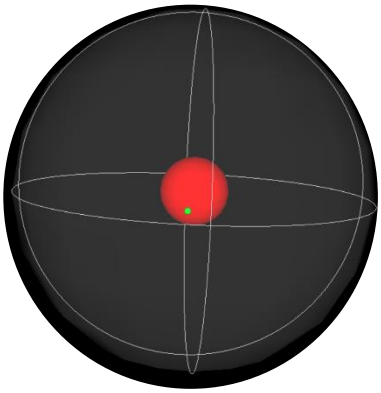

(b)

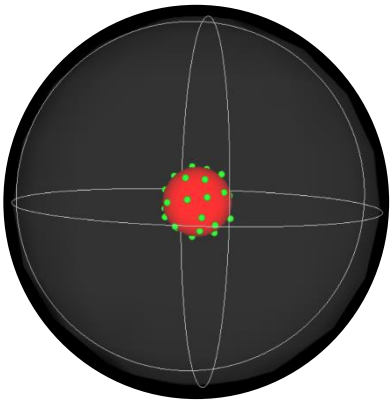

(c)

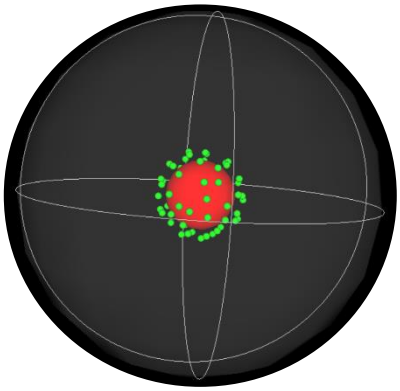

(d)

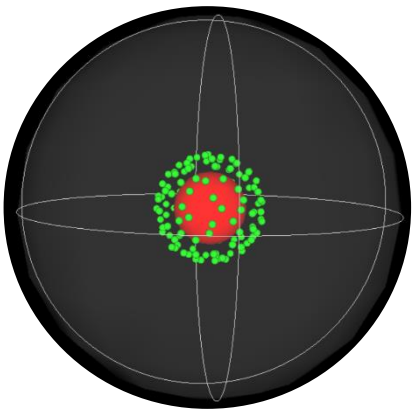

(e)

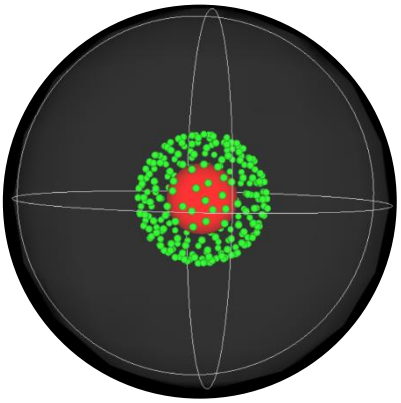

(f)

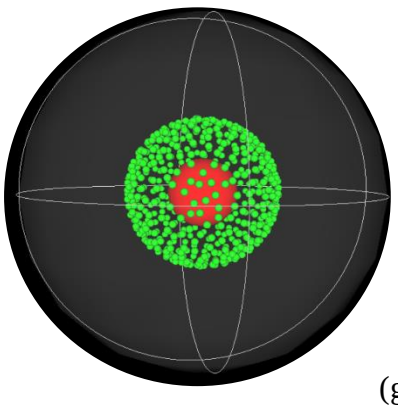

(g)

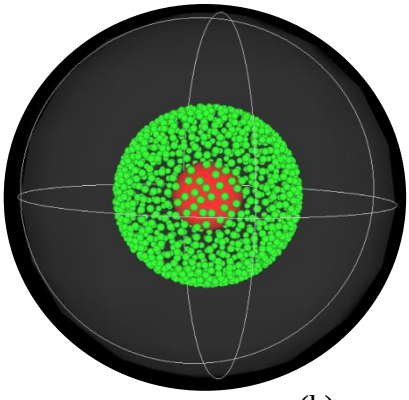

(h)

Figure 3.16: The arrangement of counterions (small balls with green color) around dendrimers (big, red balls) inside the 100Å spherical cell in water : a) G1, b) G2, c) G3, d) G4, e) G5, f) G6, g) G7, and h) G8.

Figure 3.16 demonstate the snapshots for the counterion distribution around the dendrimer surface inside the spherical cell. It is evident that as generation increased, the concentration of counterions at the dendrimer surface increased, and as generation decreased, the distribution became more obvious.

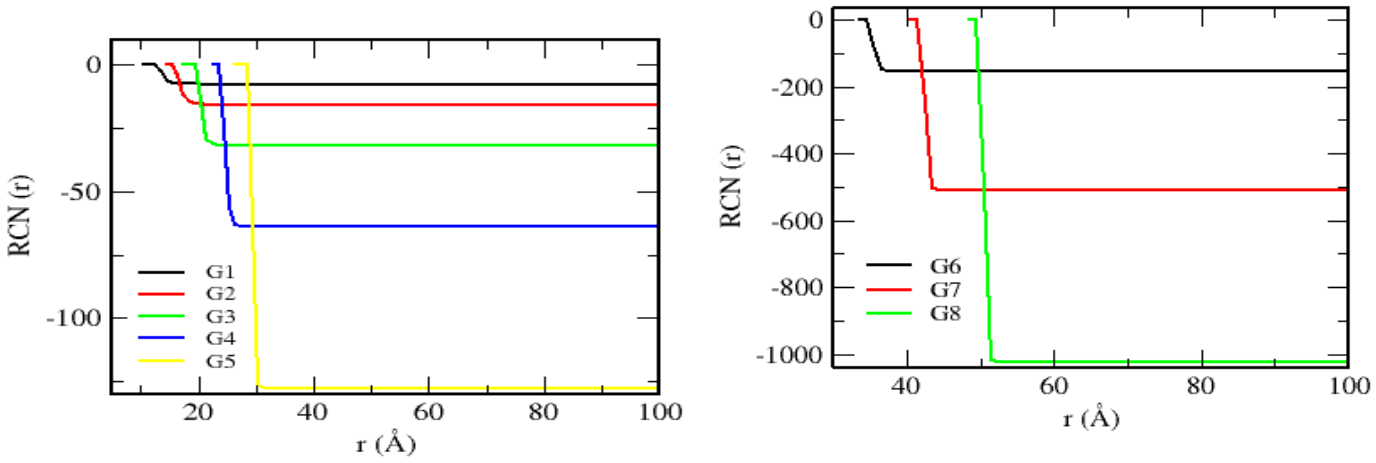

(a) (b)

Figure 3.17 (a) and (b): RCN (r) for different generations versus distance r from the dendrimer's center.

From figure 3.17, we note that the number of counterions increases as generations increase, as does the electrostatic correlation.

.

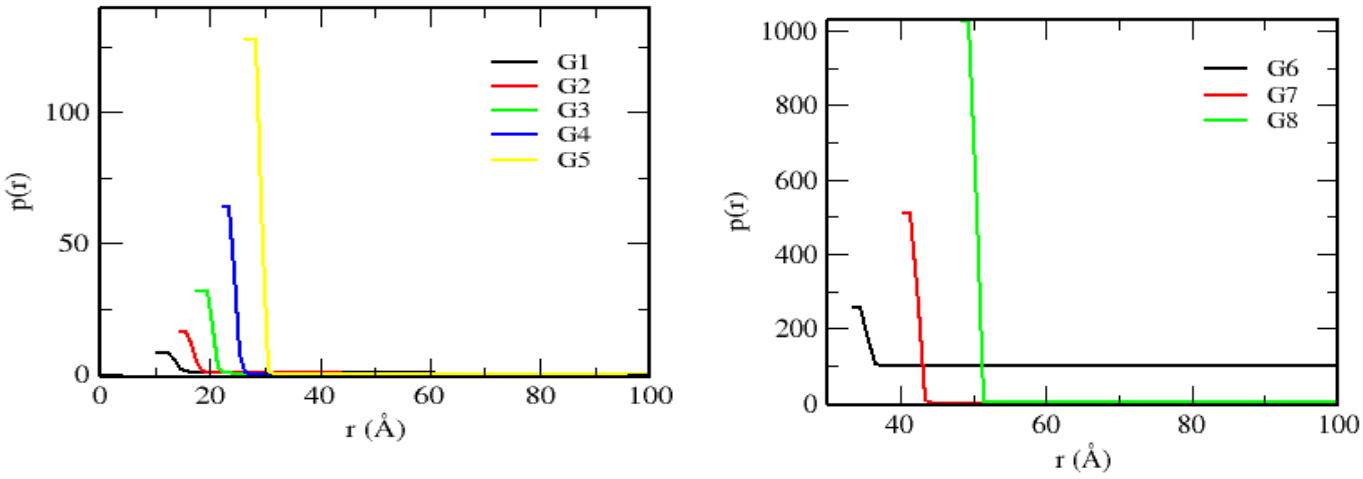

(a) (b)

Figure 3.18: (a) and (b) the integrated charge number P(r) for various generations inside the distance r from the dendrimer center.

In Figure 3.18, it is evident that as the dendrimer's generation increases, there is a noticeable increase in the accumulation of counterions near the dendrimer's surface. Additionally, the figure also illustrates that the attractive electrostatic interaction between the dendrimer and the counterions becomes stronger as the distance 'r' inside the spherical cell increases.

The electrostatic potential φ (r) of the EDL has been plotted as shown in figure 3.19 :

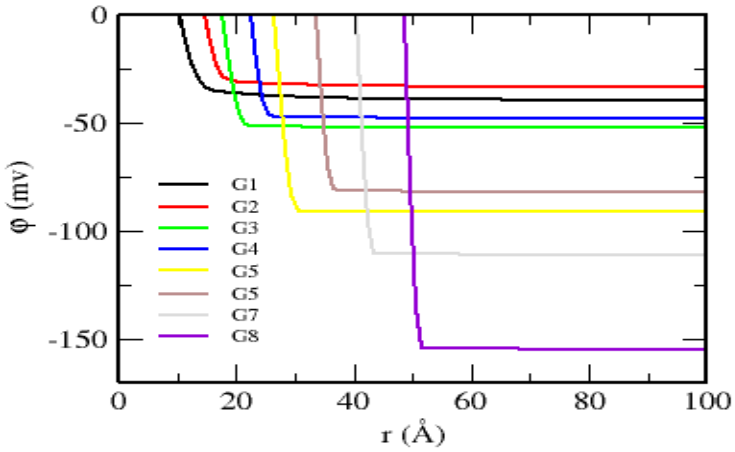

Figure 3.19 The electrostatic potential of the electric double layer represented as φ(r), within the distance from the center of the dendrimer, when the dielectric constant is 10.

According to figure 3.19, the negative magnitude of the electrostatic potential is elevated near the dendrimer's surface. This elevation is directly associated with an increase in the number of counterions, indicating that the electrostatic potential becomes stronger due to the heightened electrostatic interactions between the dendrimer and the counterions.

Figure 3.20 (a) shows the zeta potential (ζ). The values of zeta potential decrease as generation increases to reach G5, then back to get a little increase from G6 to G8, whereas the maximum value of zeta potential is reached at the highest value of G1. Figure 3.20 (b) shows that the surface electrostatic potential (φ_s) was found to be the largest on the surface of G8, and the values of the surface potential increase as the generation of the dendrimer increases.

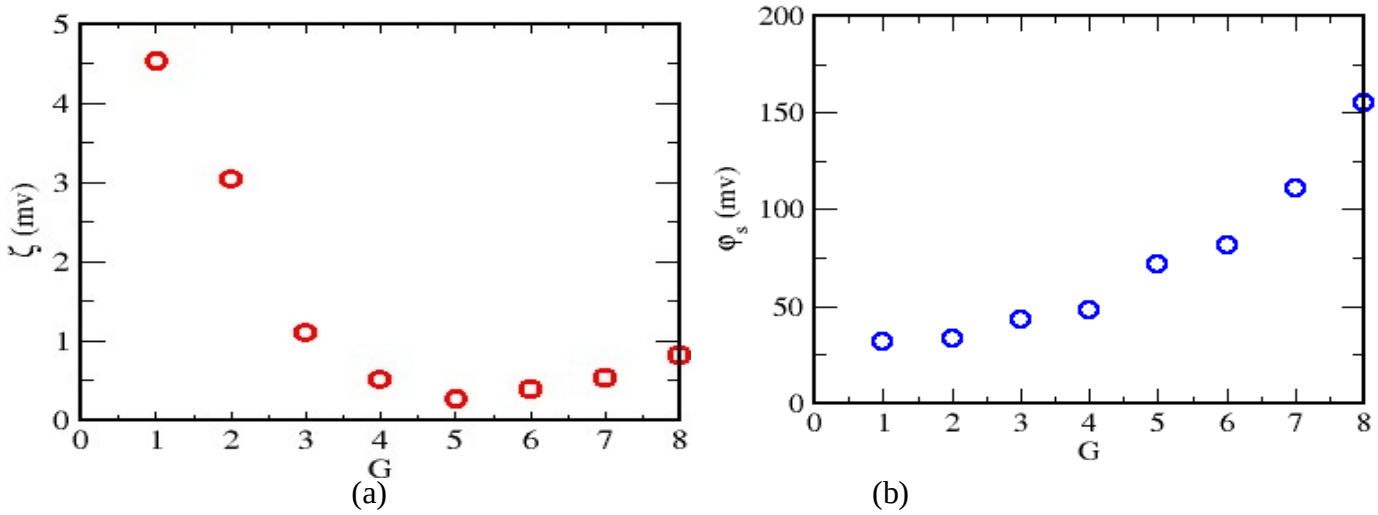

Figure 3.20: (a) Zeta potential and (b) surface potential of the dendrimer.

It is clear that the absolute values of this zeta potential decrease as the generation increases

Chapter Four

Conclusion and Recommendation

4.1 Conclusion

Monte Carlo simulation is used to study the potential of the electric double layer for dendrimers of different generations in aqueous solution and in the cytoplasm. Through the study, we worked on changing the radius of the macroion and the sphere, changing charges, and studying the effect of these changes on different dendrimers.

When the dendrimer is centered at a distance of r from the center of a solution without salt and a dielectric constant of 78.4, the radial distribution function gives the relative density of an ions at that distance. The value of this parameter is set to unity when there is no spatial correlation between different generations. Dendrimer counterions arranged near the macroion surface as a function of r show a rapid accumulation of counterions near the surface as r is increased, and the distribution increases with increasing generation. We note that the running coordination number of ions increases when generation increases, as does the electrostatic correlation, and it is the same for the integrated charge number. The accumulation of counterions around the surface of dendrimer increases with increasing generation as the attractive electrostatic interactions increase.

Due to an increase in the number of counterions and an increase in the electrostatic interaction between the dendrimer and counterions, the negative electrostatic potential is increasing near the macroion surface the dendrimer by increasing the generation radius.

The values of zeta potential increase by increasing the generation of the dendrimer with small, slow changes that become slower for some generations, and the values of surface electrostatic potential (φ_s) are larger than zeta potential. The values of surface potential increase as the generation of the dendrimer increases; they were found to be the largest on the surface of G8.

Concerning Zeffective, the values increased as generation increased, so the charge accumulation is high.

Therefore, the solvent's dielectric constant plays a significant role in the development of counterions on the dendrimer's surface. The largest accumulation occurred at low solvent dielectric constants, where the interaction between the dendrimer and the counterions increased as generation increased.

When the dielectric constant is 10 (representing the cytoplasm) and inside the spherical cell, the arrangement of counterions surrounding the dendrimer's surface increases when R gets smaller, which has the greatest value at small generation. Zeta potential values decrease as generation increases (positive values), but the surface electrostatic potential (φ) values increase with increasing generation, and counterions increase; also, the values are larger than zeta potential.

Finally, the model that has been described is appropriate for representing the complexation of DNA with dendrimer. The outcomes align with a set of computer simulations carried out by Kh. Qamhieh and coworkers. (2013)

4.2 Recommendation:

Particle size and zeta potential affect how well gene vectors are transfected. Zeta potential is a crucial physicochemical variable that influences nanoparticle stability and facilitates movement. The presence of a charged active material inside the nanoparticle's center or just on the surface can be determined using the zeta potential. Zeta potential can result in high electrostatic contact with the surface and is also a sign of how stable nanoparticle suspensions are.

We predict that further findings may be obtained in the future to investigate diverse features of EDL configuration. The modification of the dielectric constant of macroions and the dielectric constant of the solution can be achieved through the manipulation of various conditions, such as altering the temperature and introducing diverse types of salt at varying concentrations.

The current simulation analytical investigation holds significant practical implications and has the capacity to be a stimulating component for future research on electrostatic interaction in many asymmetric electrolyte solutions.

References

1. Anupa R. Menjoge; Rangaramanujam M. Kannan; Donald A. Tomalia (2010). Dendrimer-based drug and imaging conjugates: design considerations for nanomedical applications. , 15(5-6), 171–185.

2. Besteman, K., Zevenbergen, M. A. G., & Lemay, S. G. (2005). Charge inversion by multivalent ions: Dependence on dielectric constant and surface-charge density. *Physical Review E, 72*(6), 061501.

3. Clogston, J. D., & Patri, A. K. (2011). Zeta potential measurement. Characterization of nanoparticles intended for drug delivery, 63-70.

4. Derjaguin, B. (1993). A theory of interaction of particles in presence of electric double layers and the stability of lyophobe colloids and disperse systems. Progress in Surface Science, 43(1-4), 1-14.

5. Dias, A. P., da Silva Santos, S., da Silva, J. V., Parise-Filho, R., Ferreira, E. I., El Seoud, O., & Giarolla, J. (2020). Dendrimers in the context of nanomedicine. *International journal of pharmaceutics*, *573*, 118814.

6. Feng, Y., Kilker, S. R., & Lee, Y. (2020). Surface charge (zeta-potential) of nanoencapsulated food ingredients. In Characterization of nanoencapsulated food ingredients (pp. 213-241). Academic Press.

7. Honary, S., & Zahir, F. (2013). Effect of zeta potential on the properties of nano-drug delivery systems-a review (Part 1). Tropical journal of pharmaceutical research, 12(2), 255-264.

8. Honary, S., & Zahir, F. (2013). Effect of zeta potential on the properties of nano-drug delivery systems-a review (Part 2). *Tropical journal of pharmaceutical research*, *12*(2), 265-273.

9. Hunter, R. J. (2013). Zeta potential in colloid science: principles and applications (Vol. 2). Academic press.

10. Joly, L., Ybert, C., Trizac, E., & Bocquet, L. (2004). Hydrodynamics within the electric double layer on slipping surfaces. Physical review letters, 93(25), 257805.

11. Jörg Dennig; Emma Duncan (2002). Gene transfer into eukaryotic cells using activated polyamidoamine dendrimers. , 90(3-4), 339–347

12. Keerti Jain; Prashant Kesharwani; Umesh Gupta; N.K. Jain (2010). Dendrimer toxicity: Let's meet the challenge. , 394(1-2), 122–142.

13. Keiji Itaka; Kazunori Kataoka (2009). Recent development of nonviral gene delivery systems with virus-like structures and mechanisms.

14. Kesharwani, P., & Gupta, U. (Eds.). (2018). Nanotechnology-based targeted drug delivery systems for brain tumors. Academic Press.

15. Kim, Yejin; Park, Eun Ji; Na, Dong Hee (2018). Recent progress in dendrimer-based nanomedicine development. Archives of Pharmacal Research, (), – . doi:10.1007/s12272-018-1008-4

16. Lobaskin, V., & Qamhieh, K. (2003). Effective macroion charge and stability of highly asymmetric electrolytes at various salt conditions. The Journal of Physical Chemistry B, 107(32), 8022-8029.

17. Lu, Y., Zhang, E., Yang, J., & Cao, Z. (2018). Strategies to improve micelle stability for drug delivery. Nano research, 11(10), 4985-4998.

18. Ma, Y. Q. (2013). Theoretical and computational studies of dendrimers as delivery vectors. Chemical Society Reviews, 42(2), 705-727.

19. Mahfuz, A. M. U., Hossain, M. K., Khan, M. I., Hossain, I., & Anik, M. I. (2022). Smart drug-delivery nanostructured systems for cancer therapy. New trends in smart nanostructured biomaterials in health sciences.

20. Mansfield, Marc L.; Klushin, Leonid I. (1993). Monte Carlo studies of dendrimer macromolecules. Macromolecules, 26(16)

21. Naji, A., Kanduč, M., Netz, R. R., & Podgornik, R. (2011). Exotic electrostatics: Unusual features of electrostatic interactions between macroions. In Understanding Soft Condensed Matter via Modeling and Computation (pp. 265-295).

22. Nguyen, T. T., et al. "Screening of a Charged Particle by Multivalent Counterions in Salty Water: Strong Charge Inversion." The Journal of Chemical Physics, vol. 113, no. 3, July 2000, pp. 1110–25.

23. Nomani A, Haririan I, Rahimnia R, Fouladdel S, Gazori T, Dinarvand R, Omidi Y, Azizi E.Physicochemical and biological properties of self-assembled antisense/poly(amidoamine) dendrimer nanoparticles: the effect of dendrimer generation and charge ratio. Int J Nanomedicine. 2010 May 13;5:359-69.

24. P. Linse, MOLSIM,Lund University, Lund, Sweden, (2004).

25. Qamhieh, K., & Khaleel, A. A. (2014). Analytical model study of complexation of dendrimer as an ion penetrable sphere with DNA. Colloids and Surfaces A: Physicochemical and Engineering Aspects, 442, 191-198.

26. Qamhieh, K., & Linse, P. (2005). Effect of discrete macroion charge distributions in solutions of like-charged macroions. The journal of chemical physics, 123(10), 104901.

27. Raychaudhuri, S. (2008, December). Introduction to monte carlo simulation. In 2008 Winter simulation conference (pp. 91-100). IEEE.

28. Samad, A., Alam, M. I., & Saxena, K. (2009). Dendrimers: a class of polymers in the nanotechnology for the delivery of active pharmaceuticals. Current pharmaceutical design, 15(25), 2958-2969.

29. Santander-Ortega, M. J., Lozano, M. V., Uchegbu, I. F., & Schätzlein, A. G. (2016). Dendrimers for gene therapy. In Polymers and Nanomaterials for Gene Therapy (pp. 113-146). Woodhead Publishing.

30. Schiessel, H. (2003). The physics of chromatin. Journal of Physics: Condensed Matter, 15(19), R699.

31. Schneider S. Ph D.Thesis, Lund University, Sweden. 2003.

32. Sherje, Atul P.; Jadhav, Mrunal; Dravyakar, Bhushan R.; Kadam, Darshana (2018). Dendrimers: A versatile nanocarrier for drug delivery and targeting. International Journal of Pharmaceutics, 548(1), 707–720.

33. Siddall, J. N. (1983). Probabilistic engineering design. CRC Press.

34. Singh, S., Singh, G., Sehrawat, S., Rawat, P., Molugulu, N., Singh, V., ... & Kesharwani, P. (2021). Conclusion and future considerations of dendrimers. In Dendrimer-based nanotherapeutics (pp. 449-458). Academic Press.

35. Sinha, S., Jing, H., & Das, S. (2017). Charge inversion and external salt effect in semi-permeable membrane electrostatics. Journal of Membrane Science, 533, 364-377.

36. Tripathy, S., & Das, M. K. (2013). Dendrimers and their applications as novel drug delivery carriers. J. Appl. Pharm. Sci, 3(09), 142-149.

37. Tripathy, S., & Das, M. K. (2013). Dendrimers and their applications as novel drug delivery carriers. J. Appl. Pharm. Sci, 3(09), 142-149

38. Vogel, N., Retsch, M., Fustin, C. A., Del Campo, A., & Jonas, U. (2015). Advances in colloidal assembly: the design of structure and hierarchy in two and three dimensions. Chemical reviews, 115(13), 6265-6311.
Vol. 72.

39. Zhao, H., & Bau, H. H. (2009). The polarization of a nanoparticle surrounded by a thick electric double layer. Journal of colloid and interface science, 333(2), 663-671.

40. Zinchenko, A. A., & Chen, N. (2006). Compaction of DNA on nanoscale three-dimensional templates. Journal of Physics: Condensed Matter, 18(28), R453.

العنوان: إمكانات جهد زيتا لطبقة مزدوجة كهربائية للدندرامر باستخدام نظرية مونت كارلو

إعداد: اية ابراهيم موسى جعافرة

إشراف:الدكتورة خولة قمحية

الملخص

تمت دراسة التفاعلات الكهروستاتيكية بين الايون الكبير (dendrimer) والايونات الصغيرة (countrions) في نظام كروي (spherical boundary) باستخدام طريقة محاكاة مونت كارلو ، وتم تم دراسة تأثير تغير السماحية الكهربائية (dielectric constant ε) ، وتغيير الشحنة ونصف قطرالايون الكبير (macroion) من1 G الىG8 ,وقد تم إجراء جميع عمليات المحاكاة باستخدام حزمة محاكاة مونت كارلو المتكاملة (Molsim).

تم رسم التوزيع العشوائي (RDF)بين الايون الكبير والأيونات الأخرى ، وايضا تم رسم (RCN)، بالاضافة الى(pr) ,(z effective) وقيمة جهد زيتا(zeta potential) و جهد السطح (surface potrntial)

تم تحليل النتائج بالاعتماد على مكانة تراكم الايونات الصغيرة ، وكثافة الشحنة ، والجهود الكهروستاتيكية.

ونتيجة لذلك ، تزداد قيمة الشحنة المتراكمة عندما تزداد الأيونات الصغيرة بسبب زيادة عوامل الجذب. وتزداد قيم (zeta and surface potential) مع زيادة generation. في محلول مائي بدون اضافه ملح, وايضا تزداد قيمة جهود زيتا بشكل و يتم الوصول إلى القيمة القصوى للإمكانات عند قيمة عالية للسماحية الكهربائية ، حيث تسبب انخفاض ثابت السماحية الكهربائي=10اللذي يمثل السيتوبلازم في زياده عوامل الجذب الكهروستاتيكية فيكون تجمع الشحنات اكبر عند السطح مما يؤدي الى زياده قيمه جهد السطح بينما جهد زيتا يقل بزياده generation.